

Geological Society, London, Special Publications Online First

## **How the Neoproterozoic S-isotope record illuminates the genesis of vein gold systems: an example from the Dalradian Supergroup in Scotland**

Nyree J. Hill, Gawen R. T. Jenkin, Adrian J. Boyce, Christopher J. S. Sangster, David J. Catterall, David A. Holwell, Jonathan Naden and Clive M. Rice

*Geological Society, London, Special Publications*, first published November 22, 2013; doi 10.1144/SP393.9

---

**Email alerting service**

click [here](#) to receive free e-mail alerts when new articles cite this article

**Permission request**

click [here](#) to seek permission to re-use all or part of this article

**Subscribe**

click [here](#) to subscribe to Geological Society, London, Special Publications or the Lyell Collection

**How to cite**

click [here](#) for further information about Online First and how to cite articles

---

**Notes**

# How the Neoproterozoic S-isotope record illuminates the genesis of vein gold systems: an example from the Dalradian Supergroup in Scotland

NYREE J. HILL<sup>1\*</sup>, GAWEN R. T. JENKIN<sup>1</sup>, ADRIAN J. BOYCE<sup>2</sup>, CHRISTOPHER J. S. SANGSTER<sup>3</sup>, DAVID J. CATTERALL<sup>4</sup>, DAVID A. HOLWELL<sup>1</sup>, JONATHAN NADEN<sup>5</sup> & CLIVE M. RICE<sup>6</sup>

<sup>1</sup>*Department of Geology, University of Leicester, University Road, Leicester LE1 7RH, UK*

<sup>2</sup>*Scottish Universities Environmental Research Centre, Rankine Avenue, Scottish Enterprise Technology Park, East Kilbride G75 0QF, UK*

<sup>3</sup>*Scotgold Resources Limited, Upper Station, Tyndrum, Stirlingshire FK20 8RY, UK*

<sup>4</sup>*Farscape Exploration (FarEx) Botswana, Plot 431, Disaneng, Maun, PO Box 777, Botswana*

<sup>5</sup>*British Geological Survey, Keyworth, Nottingham NG12 5GG, UK*

<sup>6</sup>*Geology and Petroleum Geology, Kings College, University of Aberdeen, Meston Building, Aberdeen AB24 3UE, UK*

*\*Corresponding author (e-mail: njh35@le.ac.uk)*

**Abstract:** The genesis of quartz vein-hosted gold mineralization in the Neoproterozoic–early Palaeozoic Dalradian Supergroup of Scotland remains controversial. An extensive new dataset of S-isotope analyses from the Tyndrum area, together with correlation of the global Neoproterozoic sedimentary S-isotope dataset to the Dalradian stratigraphy, demonstrates a mixed sedimentary and magmatic sulphur source for the mineralization.  $\delta^{34}\text{S}$  values for early molybdenite- and later gold-bearing mineralization range from  $-2$  to  $+12\text{‰}$ , but show distinct populations related to mineralization type. Modelling of the relative input of magmatic and sedimentary sulphur into gold-bearing quartz veins with  $\delta^{34}\text{S}$  values of  $+12\text{‰}$  indicates a maximum of 68% magmatic sulphur, and that S-rich, SEDEX-bearing, Easdale Subgroup metasedimentary rocks lying stratigraphically above the host rocks represent the *only* viable source of sedimentary sulphur in the Dalradian Supergroup. Consequently, the immediate host rocks were not a major source of sulphur to the mineralization, consistent with their low bulk sulphur and lack of metal enrichment. Recent structural models of the Tyndrum area suggest that Easdale Subgroup metasedimentary rocks, enriched in  $^{34}\text{S}$ , sulphur and metals, are repeated at depth owing to folding, and it is suggested that these are the most likely source of sedimentary sulphur, and possibly metals, for the ore fluids.



**Gold Open Access:** This article is published under the terms of the CC-BY 3.0 license.

The Dalradian rocks of Scotland and Ireland have been extensively studied since the mid-nineteenth century (Murchison & Geikie 1861; Bailey & Macgregor 1912; Tilley 1925). The sequence is generally considered to be mid-Neoproterozoic (Cryogenian) to at least mid-Cambrian in age (Tanner & Sutherland 2007; Stephenson *et al.* 2013). However, there are only limited horizons where precise chronostratigraphy is available (Dempster *et al.* 2002; Rooney *et al.* 2011). Furthermore, correlation with other Neoproterozoic sequences is challenging, given that the Dalradian rocks have undergone polyphase deformation and regional metamorphism, locally reaching upper amphibolite grade during the Grampian Event of the Caledonian Orogeny (Oliver 2001; Stephenson *et al.* 2013). The

Neoproterozoic Era is recognized as a crucial time in Earth history, incorporating two snowball Earth events (Hoffman *et al.* 1998) coupled with large fluctuations in seawater C-, O-, Sr- and S-isotope ratios (Halverson *et al.* 2010). The increasing understanding of Neoproterozoic events and global isotope variations (Halverson *et al.* 2010; Halverson & Shields-Zhou 2011) within the evolving Earth has impacted on the understanding of the Dalradian sequence and is beginning to refine the possible chronostratigraphies, particularly through the use of stable isotope stratigraphy (Thomas *et al.* 2004; Prave *et al.* 2009; Moles *et al.* 2014).

The Dalradian sequence also hosts the UK's largest resource of gold in Northern Ireland at Curraghinalt, and its only active metal (gold) mine

at Cavanacaw (Fig. 1), with resources of 2 700 000 and 438 000 oz Au, respectively (Dalradian Resources Inc. 2012; Galantas Gold Corporation 2013). In Scotland, the Cononish deposit, near Tyndrum, hosts a JORC-compliant resource of 169 000 oz Au and 631 000 oz Ag in the combined Measured, Indicated and Inferred categories (Scotgold Resources Ltd 2012a). More widely, the Tyndrum area contains a number of gold prospects and many mineralized occurrences within a 10 km radius of Cononish (Hill *et al.* 2011; Tanner 2012). The origin and timing of mineralization in the Tyndrum area are subject to on-going debate (e.g. Curtis *et al.* 1993; Goldfarb *et al.* 2005).

The massive quartz veins which host the gold ores and other associated mineralization at Tyndrum are dominated by sulphides. Early limited work on the isotopic composition of the sulphides was interpreted to suggest a mixed sedimentary/magmatic sulphur source (Patrick *et al.* 1983, 1988; Curtis *et al.* 1993). This paper presents an extensive new S-isotope dataset for sulphides from Cononish and for newly identified occurrences of a range of

mineralization styles in the area, together with a suite of local host metasedimentary rocks. The global Neoproterozoic sedimentary sulphide S-isotope dataset is correlated with recent data for the S-isotope stratigraphy of the Dalradian Supergroup to constrain the S-isotope composition of the local sequence where data are absent. The potential input of sedimentary and igneous sulphur is modelled to investigate the sources of sulphur in the Tyndrum area mineralization. From this it is shown that the majority of the sulphur in the mineralization must be derived from the Dalradian sequence and the proportion of magmatic sulphur is likely to be low, but nevertheless genetically significant. Furthermore, it is demonstrated that the local host metasedimentary rocks are unlikely to have been the dominant source of sulphur for the gold vein mineralization; instead it was stratigraphically younger, but structurally underlying, Dalradian rocks which were the most likely source. This constrains a model for the source of metals and the fluid pathways for the development of mineralization.



**Fig. 1.** Simplified geological map of the Dalradian Supergroup in Scotland and Northern Ireland showing post-tectonic intrusions and major gold occurrences (stars). Representative dates for post-tectonic granites are provided; <sup>1</sup>Oliver *et al.* (2008); <sup>2</sup>Neilson *et al.* (2009); <sup>3</sup>Conliffe *et al.* (2010). Geology adapted from the British Geological Survey 1:625 000 scale Bedrock Geology map.

## Geological setting of the Scottish Dalradian sequence

### *Global context*

The formation of the Rodinia supercontinent (1100–1000 Ma; Kennedy *et al.* 2006) and its subsequent rifting provides the setting for the early Neoproterozoic Era. Wide-scale orogenic activity was accompanied by the drawdown of biolimiting elements, such as P, Fe and C, during weathering reactions (Lenton & Watson 2004) and an associated increase in atmospheric O<sub>2</sub>. The onset of these conditions ultimately produced changes within the biosphere that led to the development of oceanic metazoans and a primitive land biota (Knauth & Kennedy 2009; Parnell *et al.* 2010). By the mid-Neoproterozoic Era the drawdown of CO<sub>2</sub> and oxidizing atmospheric conditions caused the onset of global episodic glaciations extending to low latitudes (Hambrey & Harland 1981; Hoffman *et al.* 1998) with significant associated climate fluctuations (Knauth & Kennedy 2009). The Sturtian glacial episodes are variably constrained from 746 to 663 Ma (Condon & Bowring 2011) and the Marinoan glacial episode to a period of <10 Ma with global termination of glaciation by c. 653 Ma (Condon & Bowring 2011). The northwards drift of Laurentia relative to Gondwana at c. 570 Ma began to open the Iapetus Ocean (Cawood *et al.* 2001). The subsequent closure of the Iapetus Ocean caused the Grampian Orogenic Event during the mid-Palaeozoic (Soper & Hutton 1984; Pickering *et al.* 1988; Soper *et al.* 1992).

### *Deposition and tectonic setting*

The Dalradian sequence is bounded in Scotland by the Great Glen Fault to the north and Highland Boundary Fault to the south – both crustal-scale structures (Fig. 1). The sequence was deposited along the developing east Laurentian passive margin during a period of ocean widening (Anderton 1985). The Dalradian Supergroup has a depositional history spanning the Neoproterozoic (Cryogenian) to mid-Cambrian (Tanner & Sutherland 2007; Stephenson *et al.* 2013) and comprises marine-clastic sedimentary rocks with occasional carbonate beds and minor volcanic rocks (Stephenson *et al.* 2013). The oldest rocks are psammites and semi-pelitic schists deposited in an extensional basin, collectively called the Grampian Group (Figs 1 & 2). The overlying Appin Group is characterized by a limestone–pelite–quartzite assemblage deposited in a relatively stable shelf environment (Wright 1988). The Argyll and Southern Highland Groups, overlying the Appin Group, contain

significant black slates and graphitic schists, and an increased incidence of mafic lavas and sills, grading upwards into coarse turbidite sequences (Harris *et al.* 1978; Anderton 1985), with the Argyll Group host to locally developed stratabound exhalative mineralization (Stephenson *et al.* 2013). The upper-Appin and lower-Argyll Group stratigraphy is absent in the Tyndrum area (Fig. 2); the missing stratigraphy is represented by the Boundary Slide (formerly termed the Itlay Boundary Slide; Bailey 1922; Hutton 1979; Roberts & Treagus 1979; Tanner 2012).

### *Chronostratigraphic and biostratigraphic constraints*

The age of deposition is poorly constrained; a number of workers have advocated correlations within the existing age constraints (Fig. 2; Thomas *et al.* 2004; Prave *et al.* 2009; Rooney *et al.* 2011). The base of the Dalradian sequence is dated at a maximum age of c. 800 Ma by the presence of Knoydartian deformation in the basement rocks, combined with no evidence of pre-Caledonian mineral ages in the Dalradian Supergroup (Noble *et al.* 1996). The Leny Limestone within the Southern Highland Group is dated at 510–515 Ma (Cowie *et al.* 1972) based on the presence of the rare Mid-Cambrian trilobite *Pagetides* (Pringle 1940; Cowie *et al.* 1972). There are two radiometric dates for sedimentation within the Dalradian: U–Pb zircon has constrained the Tayvallich Volcanics, which represent the top of the Argyll Group, to  $601 \pm 4$  Ma (Dempster *et al.* 2002), and a Re–Os whole rock date on the Ballachulish Slate at  $659 \pm 9.6$  Ma is interpreted to represent deposition (Rooney *et al.* 2011).

### *Deformation and metamorphism*

The Dalradian package underwent polyphase deformation, the Grampian Event, as a result of the collision of Laurentia with an oceanic arc and the subsequent closure of the Iapetus ocean c. 480–465 Ma (Oliver 2001; Baxter *et al.* 2002; Stephenson *et al.* 2013). D1 is characterized by greenschist facies metamorphism and dominantly NE–SW-trending folds and ductile shears (Strachan *et al.* 2002). Peak metamorphism and maximum deformation occurred during continued over-thrusting recorded by D2 (Krabbendam *et al.* 1997; Crane *et al.* 2002), characterized by rotation and stacking of close to isoclinal, asymmetrical fold nappes (Strachan *et al.* 2002). Upright to SE-steeply dipping NE-trending structures dominate D3, reflecting decreasing intensity of deformation (Strachan *et al.* 2002). D4 deformation is associated with gently

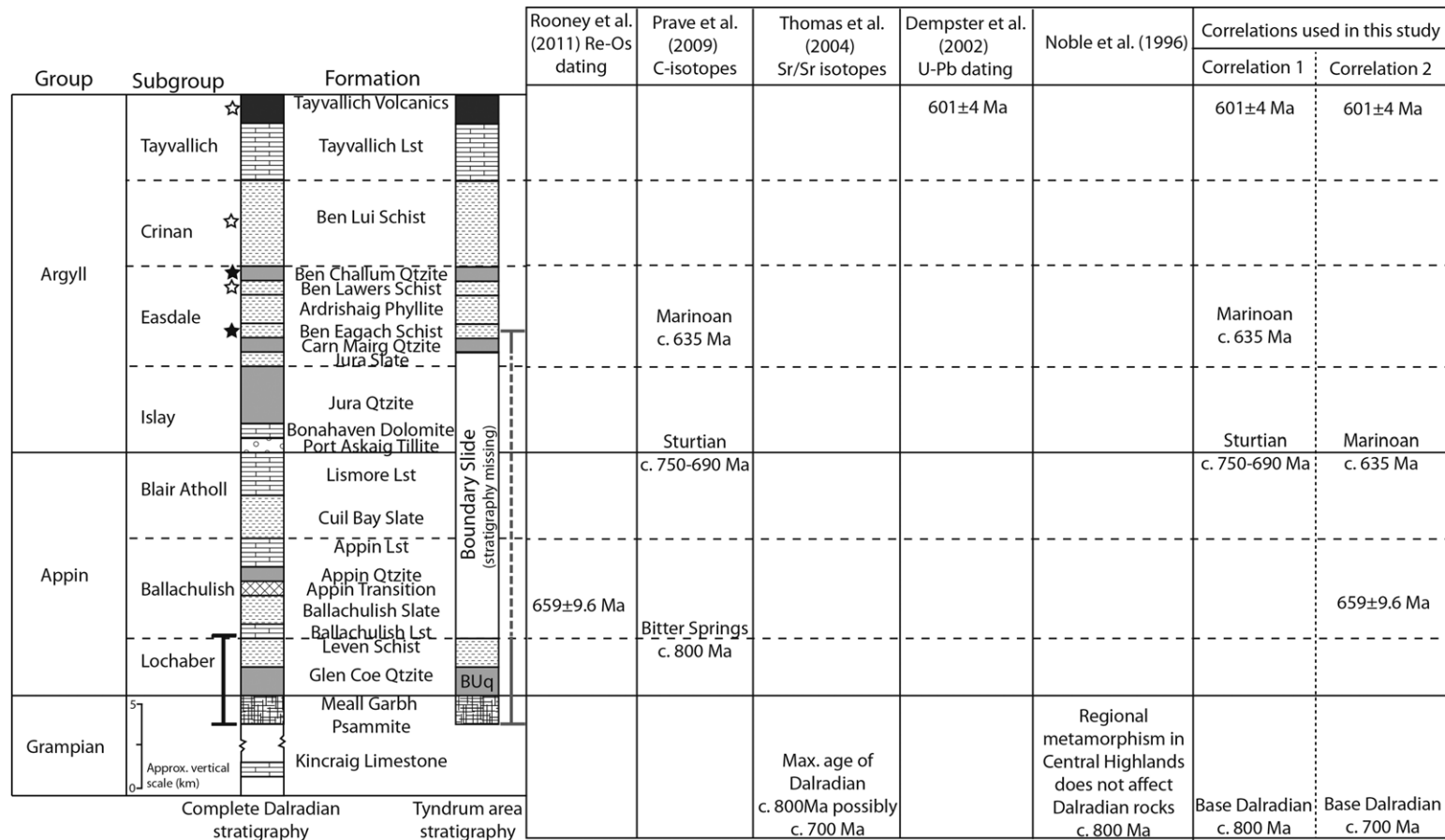


**Fig. 2.** Simplified composite stratigraphic column of the lower three groups of the Dalradian Supergroup showing missing stratigraphy in the Tyndrum area owing to the Boundary Slide. The range of host rocks for vein samples from this study is shown by the black bar with the range of host rocks for the Eas Anie structure at Cononish shown by the grey bar. The age of the Dalradian Supergroup is highly debated with limited radiometric dating available; the two age correlations used for this study are shown. Open stars indicate volcanogenic sulphide horizons; solid stars indicate syn-sedimentary stratabound SEDEX horizons. BUq, Beinn Udlaidh Quartzite (equivalent to the Glen Coe Quartzite and present in the Tyndrum area).

plunging, NE–SW-trending upright folds, late crenulation and brittle structures recording weak deformation in the final stages of the Grampian Event. Numerous faults occur sub-parallel to the NE–SW structural trend of the Dalradian, and have undergone largely left-lateral strike-slip movement with a component of normal movement during transtension (Stephenson & Gould 1995). The change to a transpressional regime is recorded by D4 and features a component of right-lateral strike-slip movement on the major Caledonian faults (Strachan *et al.* 2002). Peak metamorphism in the Dalradian Supergroup exhibits significant along-strike variation with a general increase from greenschist facies in the SW Highlands to upper amphibolite in the NE of the central Highlands (Fettes *et al.* 1985; Harte 1988). In the Tyndrum area garnet-grade amphibolite-facies metamorphism was reached (Harte 1988). Peak metamorphism is constrained to 473–465 Ma (garnet and whole rock isochron Sm–Nd; Baxter *et al.* 2002; Lu–Hf and Sm–Nd garnet and whole rock isochron; Bird *et al.* 2013) supported by the age range of broadly syn-metamorphic intrusions (Auchlee granite  $475 \pm 12$  Ma U–Pb zircon; Inch gabbro  $470 \pm 8$  Ma U–Pb zircon; Dempster *et al.* 2002; Oliver *et al.* 2008).

#### *Post-tectonic magmatic activity*

The Dalradian Supergroup hosts widespread post-tectonic granitic intrusions (Fig. 1) emplaced over a period of *c.* 25 Ma (Neilson *et al.* 2009; Conliffe *et al.* 2010). The intrusions are large granodiorite–granite multiphase complexes and range in age from the Ballachulish Complex at  $433 \pm 1.8$  Ma (Re–Os molybdenite; Conliffe *et al.* 2010) to the Etive Complex at  $408 \pm 0.4$  Ma (U–Pb zircon; Neilson *et al.* 2009), both of which host mineralization (Neilson *et al.* 2009; Conliffe *et al.* 2010; Porter & Selby 2010). Although no outcrop of granite is observed within 10 km of the Tyndrum area mineralization, a gravity low extending from the Etive Complex into the Tyndrum area has been interpreted to represent the extent of a concealed granite body (Fig. 3; Patrick *et al.* 1988). The Dalradian Supergroup also hosts intrusive bodies characterized by a significant diorite component with minor appinite/peridotite/pyroxenite (Stephenson & Gould 1995). The Garabal Hill–Glen Fyne, Arrochar and Rubha Mor appinites, 40 km south of Tyndrum, have been dated at  $426 \pm 4.2$  to  $428 \pm 9.8$  Ma (U–Pb titanite and zircon; Rogers & Dunning 1991; Tanner 2012) and are interpreted by Tanner (2012) to be equivalent to the Sron Garbh diorite–appinite body near Tyndrum and widespread lamprophyre dykes and sills observed in the Beinn Udlaidh and Glen Orchy areas (Fig. 3).

## **Isotope stratigraphy of the Dalradian Supergroup**

### *Global context*

Isotope stratigraphy has been extensively applied to Neoproterozoic sequences, in particular the correlation of glacial deposits (Halverson & Shields-Zhou 2011). Carbon-isotope stratigraphy is a powerful tool for correlating glacial deposits between Neoproterozoic sequences where there are limited biostratigraphic constraints but significant limestone deposition. Neoproterozoic carbonate sediments are characterized by high average  $\delta^{13}\text{C}_{\text{carb}}$  values and large fluctuations to extremely low values, some of which correlate with glacial episodes (Halverson *et al.* 2010). Strontium isotopes are a useful measure of tectonic evolution and long-term climatic change and are valuable in Neoproterozoic carbonate sequences owing to the consistent increase in  $^{87}\text{Sr}/^{86}\text{Sr}$  values of seawater (Halverson *et al.* 2007a). Since both C- and Sr-isotopes are measured in carbonate rocks, the two records can be tied together (Halverson & Shields-Zhou 2011). Neoproterozoic sedimentary rocks are also characterized by large fluctuations in both  $\delta^{34}\text{S}_{\text{pyrite}}$  and  $\delta^{34}\text{S}_{\text{sulphate}}$ , which appear to be closely related to glacial episodes (Gorjan *et al.* 2000; Hurtgen *et al.* 2002; Halverson & Hurtgen 2007), although the record is not as well constrained as for C- and Sr-isotope variations. In this paper, existing data on the variation of C- and Sr-isotopes within the Dalradian Supergroup are utilized, in addition to existing radiometric dating, to establish potential age correlations for the Dalradian Supergroup. This study uses the global Neoproterozoic S-isotope record in conjunction with these age correlations to estimate  $\delta^{34}\text{S}$  values in sulphur-poor stratigraphy.

### *Carbon isotopes*

Prave *et al.* (2009) compared the trend in carbonate  $\delta^{13}\text{C}$  in the Dalradian Supergroup with the global composite  $\delta^{13}\text{C}$  curve (Halverson *et al.* 2005, 2007a) and correlated observed excursions with key Neoproterozoic events. The metamorphic fluids affecting Dalradian carbonates during Grampian Event orogenesis are known to be carbon-poor; therefore, the isotopic composition of carbonate units is buffered (Holness & Graham 1995; Graham *et al.* 1997; Thomas 2000) and carbonate  $\delta^{13}\text{C}$  values are interpreted to represent primary values. Prave *et al.* (2009) tentatively correlated the Ballachulish Limestone with the *c.* 800 Ma Bitter Springs anomaly (Hill & Walter 2000; Halverson *et al.* 2007b) and the Port Askaig Tillite at the base of the Argyll Group is interpreted to represent the Sturtian glacial episodes (Fig. 2). However, it



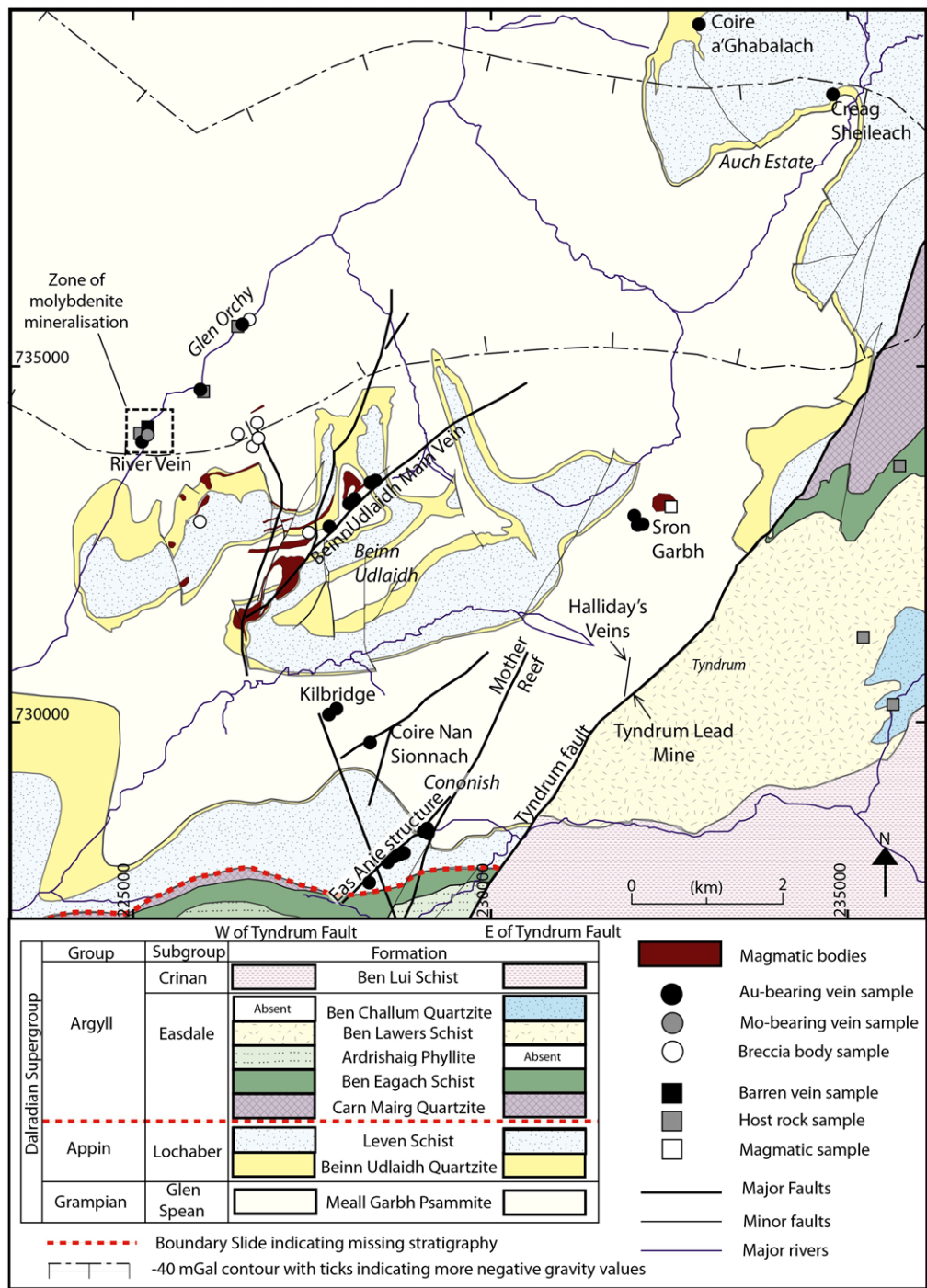


**Fig. 3.** Simplified geology of the study area. Key structural features and sample localities are shown. Magmatic bodies shown include lamprophyre sills and dykes, appinite bodies and diorite dykes. Geology adapted from the British Geological Survey 1:50 000 scale Bedrock Geology Crianlarich and Dalmally sheets with additional detail from Tanner & Thomas (2009) and mapping in conjunction with Scotgold Resources Ltd. Gravity anomaly after Hussein & Hipkin (1981) and interpretation in Patrick *et al.* (1988).

## NEOPROTEROZOIC S-ISOTOPES AND GOLD VEINS

should be noted that correlation of the Ballachulish Limestone with the Bitter Springs anomaly would make the formations below too old if it is accepted that the base of the Dalradian is <800 Ma. Prave *et al.* (2009) interpret the negative  $\delta^{13}\text{C}$  excursion in the Bonahaven Dolomite ( $\delta^{13}\text{C} = -8$  to  $-4\%$ ; Prave *et al.* 2009) to record a global depositional signal rather than local depositional variation and correlate the unit with the Tayshir anomaly within the Tsagaan Oloom Formation, Mongolia, which lies between Sturtian and Marinoan glacials (carbonate  $\delta^{13}\text{C}$  as low as  $-7.5\%$ ; MacDonald *et al.* 2009). Prave *et al.* (2009) use carbonate  $\delta^{13}\text{C}$  excursions to correlate Mid-Easdale Group units (Fig. 2) with the Marinoan glacial episode; this is supported by  $^{87}\text{Sr}/^{86}\text{Sr}$  and the presence of the Stralinchy Diamictite and overlying Cranford Limestone in the Dalradian stratigraphic sequence in NW Ireland (Thomas *et al.* 2004; McCay *et al.* 2006).

### Strontium isotopes

Thomas *et al.* (2004) used  $^{87}\text{Sr}/^{86}\text{Sr}$  values from limestones within the Dalradian Supergroup to constrain depositional age through comparison with the global  $^{87}\text{Sr}/^{86}\text{Sr}$  trend (Kuznetsov 1998, given in Shields 1999; Walter *et al.* 2000; Melezhik *et al.* 2001).  $^{87}\text{Sr}/^{86}\text{Sr}$  values for Grampian and Appin limestones are interpreted to be well preserved and therefore to represent primary values close to contemporaneous seawater. The level of preservation in the Argyll Group is less than that observed in the Grampian and Appin Group and  $^{87}\text{Sr}/^{86}\text{Sr}$  values are inferred to be less reliable. Thomas *et al.* (2004) conclude that  $^{87}\text{Sr}/^{86}\text{Sr}$  values observed in the lower Dalradian Supergroup (Kincraig Limestone, Grampian Group;  $^{87}\text{Sr}/^{86}\text{Sr} = 0.7069$ – $0.7074$ ) suggest it is not older than *c.* 800 Ma and may be as young as 700 Ma using Kuznetsov's (1998) Neoproterozoic seawater  $^{87}\text{Sr}/^{86}\text{Sr}$  curve. Comparison of the Thomas *et al.* (2004) data with the more recent Halverson *et al.* (2010) global  $^{87}\text{Sr}/^{86}\text{Sr}$  curve of high-quality Sr-isotope data supports this interpretation for the age of the Dalradian; global  $^{87}\text{Sr}/^{86}\text{Sr}$  does not increase to 0.7069 until 775 Ma when it decreases again before consistently increasing after 700 Ma. This suggests that the Dalradian Supergroup is not older than *c.* 775 Ma and may be as young as 700 Ma, in line with the geochronometric constraints that the basement is <800 Ma (Noble *et al.* 1996).

### Mineralization in the Tyndrum area

The Cononish gold mineralization is hosted in the <6 m wide Eas Anie structure, a complex of steeply dipping quartz veins, which cross-cuts Grampian and lower-Appin Group stratigraphic units (Fig. 3;

Treagus *et al.* 1999; Tanner 2012). The sulphide assemblage is dominated by pyrite, chalcopyrite and galena; gold, as electrum, is associated with galena in fractured pyrite (Earls *et al.* 1992). Previous Ar–Ar and K–Ar dating suggests that mineralization occurred at  $410 \pm 14$  Ma (Treagus *et al.* 1999), significantly after peak metamorphism and overlapping with granite magmatism, but with very large uncertainties. Recent geochronological work also suggests the age of mineralization is close to 410 Ma (Rice *et al.* 2012).

The Beinn Udlaidh Main Vein (Fig. 3) is hosted in Meall Garbh Psammite, Beinn Udlaidh Quartzite (regionally equivalent to the Glen Coe Quartzite) and Leven Schists; it trends NE, dips sub-vertically and averages 4 m in width (Fig. 3; Tanner 2012). The Main Vein contains gold, as electrum, hosted within pyrite; galena and sphalerite are present (Plewe 2012).

Previous work in the Tyndrum area noted a number of gold-bearing veins in addition to the Cononish and Beinn Udlaidh veins (Fig. 3). Halliday's Veins were first reported by Halliday (1962), with further work by Patrick *et al.* (1988). The veins, hosted in north-trending structures, contain electrum and hessite ( $\text{Ag}_2\text{Te}$ ) with minor sylvanite ( $[\text{AuAg}]_2\text{Te}_4$ ) and petzite ( $\text{Au}_3\text{AgTe}_2$ ) (Patrick *et al.* 1988). Electrum is the most common Au–Ag phase and is found as inclusions in galena and within fractures in pyrite (Patrick *et al.* 1988). Mineralized veins at Coire Nan Sionnach were noted by Earls *et al.* (1992) with additional veins observed at Kilbridge by Scotgold. The Mother Reef, sub-parallel to the Tyndrum Fault, can be traced for 2 km and is interpreted to represent a series of segments at an oblique trend to the main structure; it is largely barren except where the projected line of Eas Anie meets the Mother Reef (Tanner 2012). The Tyndrum Lead Mine mineralization is hosted in NE-trending structures within the Tyndrum Fault zone as veins and vein breccias. The sulphide assemblage is dominated by galena and sphalerite with a notable absence of pyrite (Patrick *et al.* 1983). Mineralization with a comparable assemblage is observed to cross-cut the gold-bearing Eas Anie structure (Earls *et al.* 1992).

### Previous S-isotope data

A number of S-isotope studies have previously been undertaken on veins and other mineralization styles across the Tyndrum area, and are summarized in Figure 4. Curtis *et al.* (1993) undertook initial S-isotope work at Cononish, producing a limited dataset (pyrite  $\delta^{34}\text{S} = +6.0$  to  $+8.4\%$ ;  $n = 9$ ) interpreted to reflect a mixture of magmatic and sedimentary sources, although the dataset did not examine variation among the different sulphide



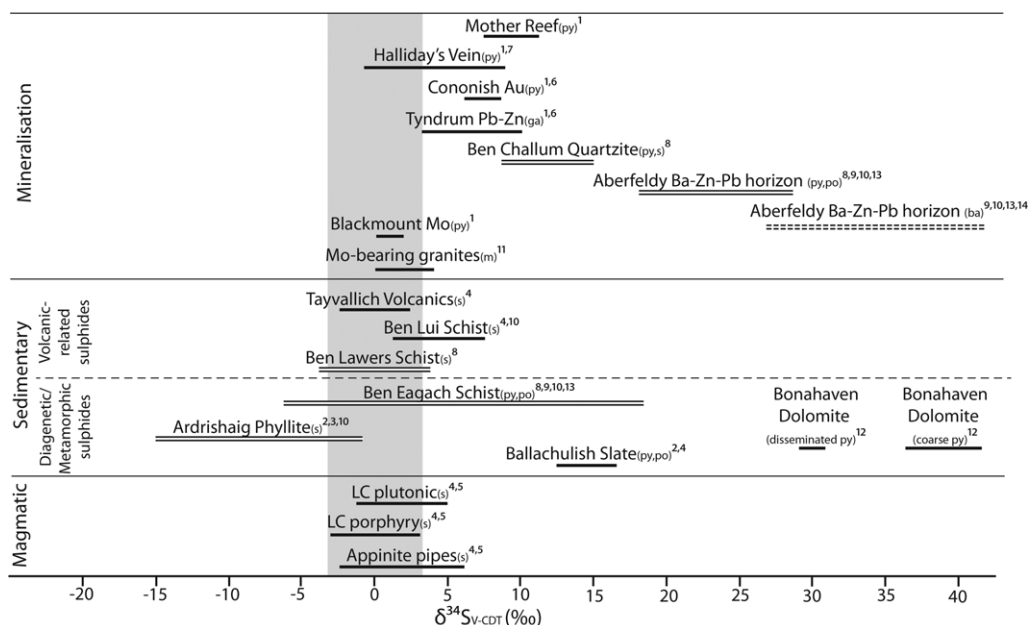


**Fig. 4.** Previous sulphide and sulphate  $\delta^{34}\text{S}$  data for sedimentary, magmatic bodies and mineralization in the Dalradian Supergroup. Grey bar represents  $\delta^{34}\text{S}$  range for uncontaminated mantle-derived magmatic melts ( $\delta^{34}\text{S} = 0 \pm 3\text{‰}$ ; Ohmoto 1986). Dashed line represents sulphate  $\delta^{34}\text{S}$  data. Double lines represent Easdale Subgroup stratigraphy. <sup>1</sup>Curtis *et al.* (1993); <sup>2</sup>Hall *et al.* (1988); <sup>3</sup>Hall *et al.* (1994a); <sup>4</sup>Lowry (1991); <sup>5</sup>Lowry *et al.* (1995); <sup>6</sup>Patrick *et al.* (1983); <sup>7</sup>Patrick *et al.* (1988); <sup>8</sup>Scott *et al.* (1987); <sup>9</sup>Scott *et al.* (1991); <sup>10</sup>Willan & Coleman (1983); <sup>11</sup>Conliffe *et al.* (2009); <sup>12</sup>Hall *et al.* (1994b); <sup>13</sup>Moles *et al.* (2014); <sup>14</sup>Hall *et al.* (1987). LC, Late Caledonian; ba, barite; ga, galena; m, molybdenite; py, pyrite; po, pyrrhotite; s, sulphides.

generations observed in the vein. In addition, Patrick *et al.* (1983, 1988) and Curtis *et al.* (1993) measured values on a limited number of samples (Figs 3 & 4) from the gold-bearing Halliday's Veins (pyrite  $\delta^{34}\text{S} = -0.6$  to  $+8.8\text{‰}$ ; galena  $\delta^{34}\text{S} = +1.5$  to  $+2.0\text{‰}$ ;  $n = 6$ ) and the largely barren Mother Reef (pyrite  $\delta^{34}\text{S} = +8.0$  to  $+9.8\text{‰}$ ; galena  $\delta^{34}\text{S} = +7.2$  to  $+11.2\text{‰}$ ;  $n = 7$ ). Patrick *et al.* (1983) and Curtis *et al.* (1993) measured S-isotopes of galena ( $\delta^{34}\text{S} = +3.5$  to  $+6.6\text{‰}$ ;  $n = 10$ ) and sphalerite ( $\delta^{34}\text{S} = +6.6$  to  $+10.0\text{‰}$ ;  $n = 3$ ) from the Tyndrum Lead Mine (Figs 3 & 4). Molybdenite  $\delta^{34}\text{S}$  data from mineralization at Ballachulish and Etive ranges from 0 to  $+4\text{‰}$  (Conliffe *et al.* 2009) and pyrite  $\delta^{34}\text{S}$  values from Blackmount molybdenite veins (Etive Complex;  $n = 2$ ; Fig. 1) are close to zero (Curtis *et al.* 1993).

The range of data for the different mineralization styles as displayed in Figure 4 shows that different mineralization types have distinct S-isotope signatures. Sulphide  $\delta^{34}\text{S}$  data from all mineralization types are generally positive with only rare values below  $0\text{‰}$ . Gold mineralization is associated with  $\delta^{34}\text{S}$  ratios in the range  $-0.6$  to  $+9.8\text{‰}$  with an average of  $6.3\text{‰}$  ( $\pm 2.8\text{‰}$   $\sigma_{n-1}$ ) for pyrite.

Molybdenite mineralization has  $\delta^{34}\text{S}$  values close to zero, suggesting it is magmatic in origin and is comparable with  $\delta^{34}\text{S}$  data from deep-seated plutonic intrusions across the area (average  $\delta^{34}\text{S} = +2.6 \pm 1.8\text{‰}$ ; Lowry *et al.* 1995; Fig. 4).

### Analytical methods

Samples were obtained from surface and underground outcrop and quarter drill core from Scotgold Resources Ltd's on-going exploration programme. Detailed mineralogical analysis was undertaken at the University of Leicester using a Hitachi S-3600N environmental scanning electron microscope, with an Oxford Instruments INCA 350 energy-dispersive X-ray analysis system. Whole rock geochemistry was undertaken at ALS laboratories, Ireland, as part of Scotgold's assay programme; only sulphur and gold concentrations are reported here. For sulphur, samples were dissolved in concentrated perchloric, nitric, hydrofluoric and hydrochloric acids. Sulphur was analysed by ICP-MS; the lower detection limit was  $0.01\%$ . Gold was measured by fire assay, fusing the sample with lead oxide, sodium carbonate, borax

## NEOPROTEROZOIC S-ISOTOPES AND GOLD VEINS

and silica then digesting the bead in dilute nitric and hydrochloric acid. The digested solution was analysed by atomic absorption; the lower detection limit was 0.01 ppm.

Sulphide minerals for S-isotope analysis were separated using micro-drilling from characterized sections. SO<sub>2</sub> was produced from sulphides by combustion with cuprous oxide for mass spectrometric analysis following the procedure of Robinson & Kusakabe (1975). *In situ* laser combustion analyses were undertaken on polished slabs from the Auch Estate, prepared using a method as described in Kelley & Fallick (1990) and Wagner *et al.* (2002). For both sulphur isotope methods mass spectrometric analysis was undertaken in a VG SIRA II gas mass spectrometer. Reproducibility, based on repeat analyses of internal and international laboratory standards (CP1, NBS 123 & IAEA S 3), was better than  $\pm 0.3\%$ . All data are reported as  $\delta^{34}\text{S}$  per mil (‰) relative to the Canyon Diablo Troilite standard (V-CDT).

### Field relations of newly identified mineralization

Regional exploration by Scotgold since 2007 and work in this study have identified a number of additional occurrences of veins and clarified that mineralization is of a number of distinct types:

- (1) Additional gold-bearing quartz veins have been identified in the Glen Orchy area, at Kilbridge and the Auch Estate (Fig. 3). Steeply dipping gold-bearing quartz veins in the Glen Orchy area (up to 194.6 g/t Au and >200 g/t Ag from >1 kg grab samples; Scotgold Resources Ltd 2011a) trend east–west to SW–NE, reaching up to 1 m in width. The veins are polyphase and exhibit brecciation with host rock clasts included in the veins. Mineralized quartz veins at Kilbridge, trending 095–125 and reaching 20 cm in width, are characterized by fine-grained pyrite concentrated in a zone, up to 3 cm wide, in the centre of the vein. Auch Estate gold-bearing quartz veins (up to 25.5 g/t Au and 14.3 g/t Ag over 1 m; Scotgold Resources Ltd 2011b) are up to 0.5 m in width and trend NE–SW to ENE–WSW. Coire a'Ghabalach veins (Fig. 3) exhibit significant brecciation with clasts of early white quartz and altered host rock in the vein. Veins at Creag Shieleach are characterized by a simple sulphide assemblage and exhibit a lack of brecciation compared with other veins in the Auch Estate (Fig. 3).
- (2) Barren quartz veins are observed throughout the study area (Fig. 3) and can be characterized

into two sub-types: pyrite-free and pyrite-bearing. Pyrite-free veins are often massive and complex (e.g. Mother Vein at Cononish; Curtis *et al.* 1993; Treagus *et al.* 1999). Pyrite-bearing barren veins are characterized by a single quartz generation with some brecciation of altered host rock within the veins.

- (3) In Glen Orchy disseminated molybdenite mineralization (up to 2.72% Mo from rock chip samples; Scotgold Resources Ltd 2012c) has been identified in alteration zones around steeply dipping NNE-trending fractures. The alteration zones are up to 20 cm wide, but the fractures are narrow (millimetre scale), except where late quartz and pyrite infill has occurred (reaching up to 10 cm in width). Molybdenite occurs as small rosettes (1–2 mm across) with minor pyrite; there is no gold associated with the molybdenite mineralization.
- (4) Gold-mineralized breccia bodies have been identified at Beinn Udlaidh (up to 0.26 g/t Au and 1.49 g/t Ag over 14 m; Scotgold Resources Ltd 2010). The breccia bodies have a sharp, near vertical, contact with the host rock where observed (Moore 2011) and are approximately circular in cross-section, reaching 120 m in diameter (Tanner 2012). The breccia bodies are matrix poor owing to the close fit of angular clasts of host quartzite, psammite, schist and lamprophyre; the matrix consists of either lamprophyre or quartz (Moore 2011). The breccia bodies exhibit strong similarities to explosion breccia bodies related to appinites (Wright & Bowes 1968) and Tanner (2012) has interpreted the emplacement of the breccia bodies to have occurred syn- to post-emplacement of the lamprophyres and appinites based on cross-cutting relationships.
- (5) A platinum group element-bearing appinitic-diorite intrusive body has been identified at Sron Garbh (up to 0.22 g/t Au; 0.78 g/t Pd and 0.58 g/t Pt over 2 m; Scotgold Resources Ltd 2012b; Fig. 3); platinum group element are associated with the marginal appinite (Scotgold Resources Ltd 2012b).

In the Glen Orchy area all newly identified veins and breccia bodies cross-cut the metamorphic fabric and therefore post-date peak metamorphism. Cross-cutting relationships constrain gold-bearing quartz veins and pyrite-bearing barren veins to be younger than the molybdenite mineralization (Fig. 5). In addition, gold-bearing quartz veins are observed to cross-cut the Sron Garbh appinite. There are currently no geochronological data for Glen Orchy to constrain age relationships and absolute timescale further and therefore this study assumes,

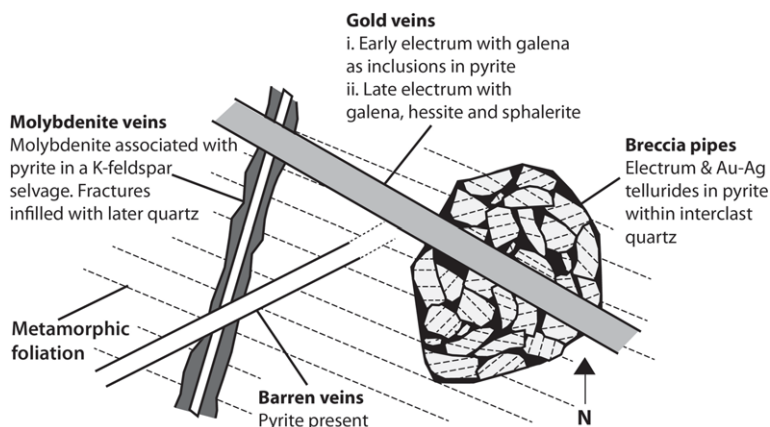


**Fig. 5.** Schematic illustration of orientations and cross-cutting relationships of the veins and breccia pipes in Glen Orchy.

in the absence of evidence otherwise, that all gold mineralization is of the same age. However, based on structural relationships, Tanner (2012) has interpreted gold mineralization at Cononish to be older than gold mineralization at Glen Orchy.

## Ore petrography

Additional work at Cononish has clarified the paragenesis compared with previously published data (Patrick *et al.* 1988; Earls *et al.* 1992; Curtis *et al.* 1993). Early gold (Au 1) is associated with hessite ( $\text{Ag}_2\text{Te}_2$ ) with minor early galena and is found in fractures in pyrite. Late gold (Au 2) is associated with galena and chalcopryrite with minor sphalerite (Spence-Jones 2013); no telluride mineralization is observed associated with late galena.

Gold-bearing quartz veins in Glen Orchy, Beinn Udlaidh, Sron Garbh, Kilbridge and Coire Nan Sionnach (Fig. 3) are characterized by a sulphide-assemblage dominated by pyrite and galena. Brecciation of adjacent host rock is observed with clasts altered to either K-feldspar or a chlorite-sericite assemblage. Early gold (Au 1) is associated with galena as inclusions in pyrite (Fig. 6a, b). A second phase of gold (Au 2) occurs with void-filling galena (Fig. 6d, e) often accompanied by sphalerite exhibiting chalcopryrite disease (Fig. 6c), and sporadic hessite. Gold-bearing veins in the Auch Estate (Fig. 3) have a comparable sulphide assemblage with the addition of arsenopyrite (Fig. 6h). Brecciation of the host rock and early white quartz is observed. Arsenopyrite forms syn-pyrite and electrum is hosted as inclusions within both arsenopyrite and pyrite and within fractures in pyrite. The veins at Coire a'Ghabalach (Fig. 3) have late void-filling galena with hessite, sphalerite (Fig. 6f, g) and

occasional Au–Ag tellurides and altaite ( $\text{PbTe}$ ); veins at Creag Sheileach (Fig. 3) have late galena, but no associated telluride mineralization.

Mineralization in breccia bodies is hosted in the quartz matrix and is associated with post-brecciation sericite–chlorite alteration of the clasts. Gold, in the form of Au–Ag tellurides, is found within pyrite with altaite ( $\text{PbTe}$ ) and sporadic chalcopryrite and galena (Moore 2011).

Sulphides in lamprophyre sills are characterized by small (<5 mm wide) cubic pyrite; no other sulphides are observed. Mineralization has been identified in the Sron Garbh appinite–diorite body; the assemblage is dominated by pyrite and chalcopryrite with platinum group minerals associated with the appinitic portion (Graham 2013).

## S-isotope results

Pyrite  $\delta^{34}\text{S}$  values from gold-bearing quartz veins obtained for this study ( $n = 46$ ) show wide variation from  $-2$  to  $+12\text{‰}$  (Fig. 7; Table 1) with an average value of  $+6.9\text{‰}$  ( $\pm 2.9\text{‰}$   $\sigma_{n-1}$ ), very similar to the  $\delta^{34}\text{S}$  of sulphide float concentrate from crushed bulk ore at Cononish of  $+6.7\text{‰}$ . All pyrite  $\delta^{34}\text{S}$  values at Cononish are pre-Au 1; galena, sphalerite and chalcopryrite  $\delta^{34}\text{S}$  values are syn-Au 2 and overall follow the same distribution as pyrite  $\delta^{34}\text{S}$  values. New data from veins at the Cononish deposit record a much wider range of values ( $\delta^{34}\text{S} = -2$  to  $+11\text{‰}$ ; Fig. 7a) than reported by Curtis *et al.* (1993). The majority of  $\delta^{34}\text{S}$  data recorded for gold-bearing quartz veins at Glen Orchy, Sron Garbh and Beinn Udlaidh (Fig. 3) are within the range of previously published work from Cononish (Curtis *et al.* 1993; Figs 4 & 7a);  $\delta^{34}\text{S}$  values below  $+5\text{‰}$  are only observed at



## NEOPROTEROZOIC S-ISOTOPES AND GOLD VEINS

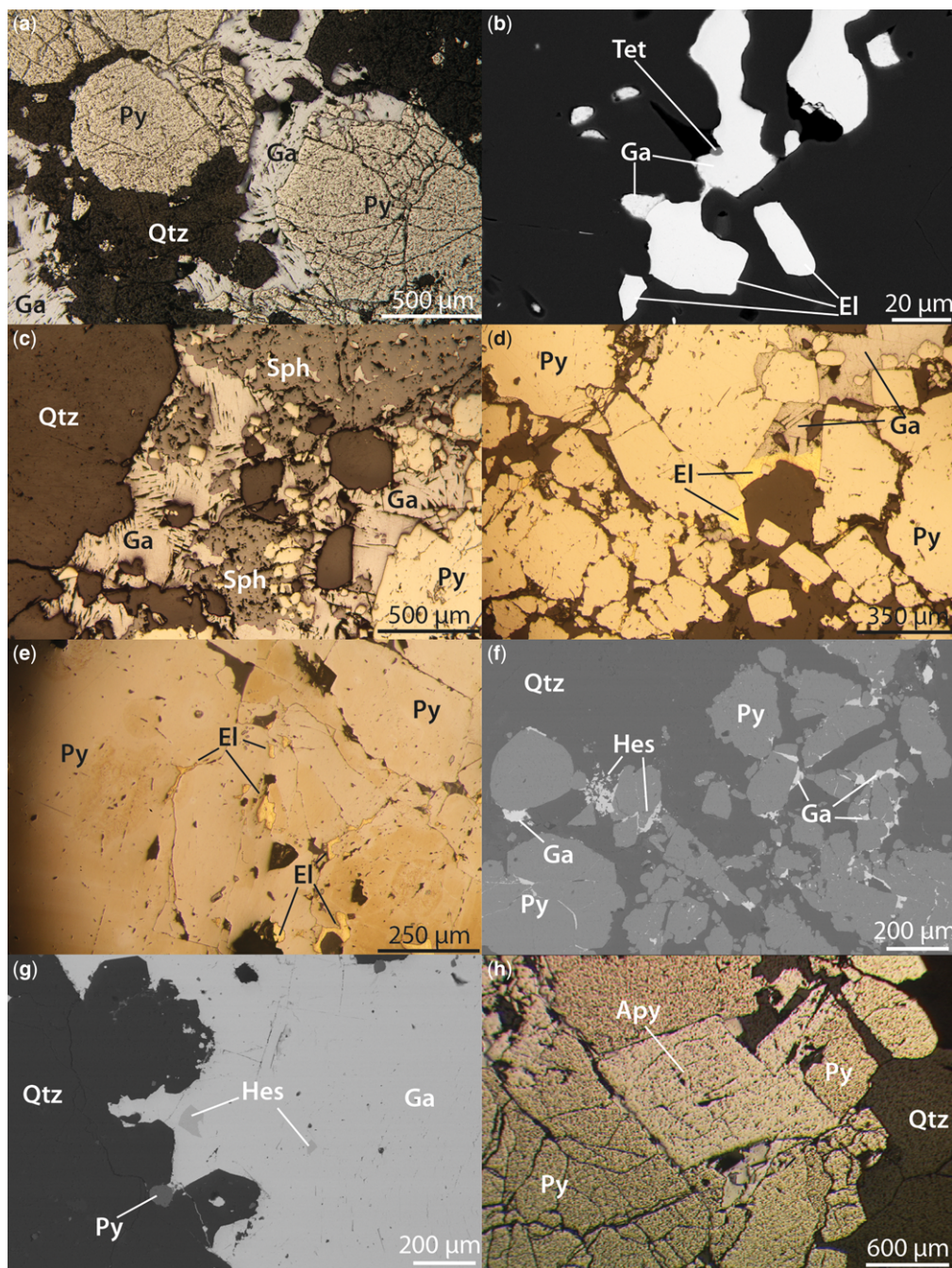


**Fig. 6.** (a) Early well-developed pyrite cross-cut by late void-filling galena. (b) Gold 1 with early galena and tetrahedrite hosted within well-developed early pyrite. (c) Extensive sphalerite development with late void-filling galena. (d) Electrum (Au 2) observed on edges of pyrite with void-filling galena. (e) Gold 2 as electrum in fractures in early pyrite. (f, g) Hessite ( $\text{Ag}_2\text{Te}$ ) associated with void filling galena forming on the edges of and within fractures in pyrite. (h) Well-developed diamond shaped crystals of arsenopyrite with pyrite. Images a–e are from Glen Orchy; f–h are from the Auch Estate. Images a, c–e, h are reflected light photomicrographs; b, f–g are SEM images. El, electrum; Py, pyrite; Ga, galena; Qtz, quartz; Sph, sphalerite; Apy, arsenopyrite; Tet, tetrahedrite; Hes, hessite.

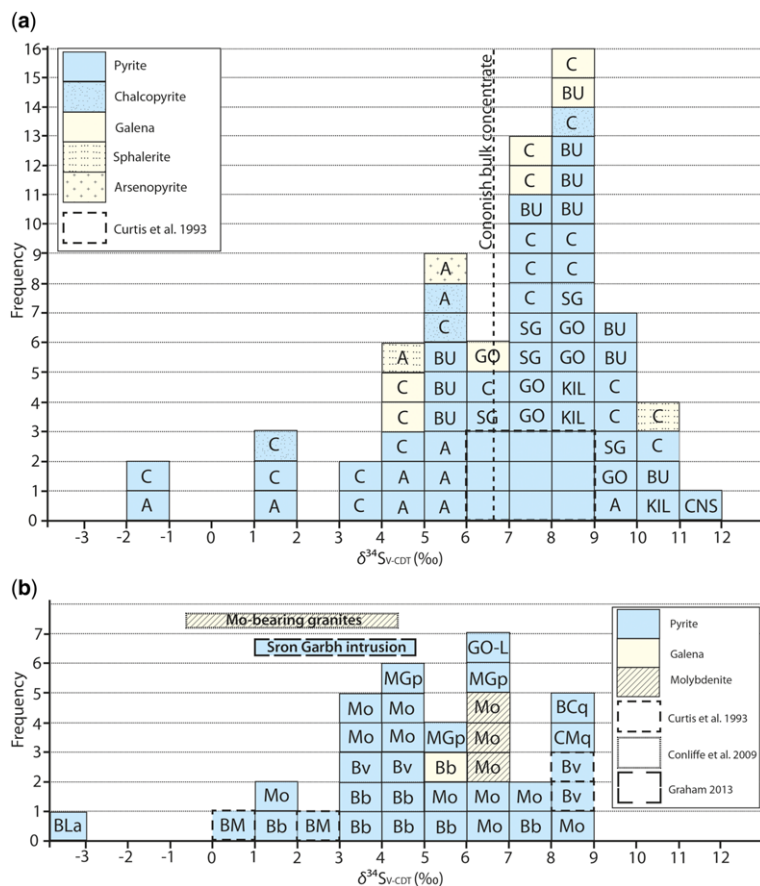


**Fig. 7.** New S-isotope data for different mineralization types, intrusions and host rocks in the Tyndrum area. **(a)** S-isotope data for gold-bearing quartz veins in the Tyndrum area. Cononish bulk concentrate represents the  $\delta^{34}\text{S}$  value measured for sulphide float concentrate from crushed bulk ore. **(b)** S-isotope data for breccia bodies, barren veins, molybdenite mineralization, magmatic bodies and host rocks. A, Auch Estate; BM, Blackmount; BU, Beinn Udlaidh; C, Cononish; CNS, Coire Nan Sionnach; KIL, Kilbridge; GO, Glen Orchy (Au-bearing quartz veins); GO-L, Lamprophyre from Glen Orchy; SG, Sron Garbh; Bb, Breccia bodies at Beinn Udlaidh; Bv, Barren Veins; Mo, Molybdenite-related; MGp, Meall Garbh Psammite; CMq, Carn Mairg Quartzite; BCq, Ben Challum Quartzite; BLA, Ben Lawers Schist.

Cononish and in the Auch Estate veins. Kilbridge and Coire Nan Sionnach (Fig. 3) exhibit slightly higher  $\delta^{34}\text{S}$  values between +8 and +12 ‰. Pyrite  $\delta^{34}\text{S}$  values are generally syn- to post-Au 1 and arsenopyrite  $\delta^{34}\text{S}$  values are post-Au 1; galena, sphalerite and chalcopyrite  $\delta^{34}\text{S}$  values are syn-Au 2. Data obtained for Tyndrum Lead Mine-type mineralization at Cononish (Table 1) are comparable to data from the Tyndrum Lead Mine (Patrick *et al.* 1983; Curtis *et al.* 1993).

Beinn Udlaidh breccia bodies (Fig. 3) record  $\delta^{34}\text{S}$  values of +1 to +8 ‰ ( $n = 8$ ; Fig. 7b). Pyrite from molybdenite-bearing fractures has  $\delta^{34}\text{S}$  values of between +1.8 and +8.4 ‰ ( $n = 10$ ), higher than pyrite  $\delta^{34}\text{S}$  values obtained at Blackmount (Curtis *et al.* 1993). Molybdenite  $\delta^{34}\text{S}$  values

measured ( $\delta^{34}\text{S} = +6$  to 6.6 ‰;  $n = 3$ ; Fig. 7b) are significantly higher than recorded for molybdenite elsewhere in the region.

Mineralized lamprophyre from Glen Orchy, taken at the contact with a cross-cutting gold-bearing quartz vein (GO1213, Table 1), has a  $\delta^{34}\text{S}$  value of +6.7 ‰. Sron Garbh appinite–diorite body (Fig. 3) has  $\delta^{34}\text{S}$  values of +1 to +4.8 ‰ (Fig. 7b; Graham 2013).

A limited S-isotope dataset has been developed for the metasedimentary rocks in the study area ( $n = 6$ ; Fig. 7b; Table 1). The host rocks are generally sulphur-poor and measured  $\delta^{34}\text{S}$  values are from a range of sulphide types: stratabound sedimentary exhalative (SEDEX) mineralized horizons (Ben Challum Quartzite), volcanogenic sulphides



**Table 1.** *S-isotope results from mineralization, sedimentary and magmatic sulphide showings in the Tyndrum area*

|                    | Location       | Vein              | ID number     | X coordinate | Y coordinate | Z coordinate (m) | Sample type | Description  | Species      | Yield (%) | $\delta^{34}\text{S}$ (‰) |
|--------------------|----------------|-------------------|---------------|--------------|--------------|------------------|-------------|--|--------------|-----------|---------------------------|
| Gold-bearing veins | Auch Estate    | Creag Sheileach   | A01a          | 234779       | 738791       | 399              | Hand sample | Pyrite in brecciated quartz vein (post Au 1)                               | Pyrite       | 87        | 9.56                      |
|                    |                |                   | A01b          | 234779       | 738791       | 399              | Hand sample | Massive pyrite between late quartz veins (post Au 1)                       | Pyrite       | 73        | 5.56                      |
|                    |                | Coire a'Ghabalach | CG01B1        | 232890       | 739788       | 666              | Hand sample | Massive pyrite containing galena inclusions in brecciated zone (post Au 1) | Pyrite       | 60        | 1.40                      |
|                    |                |                   | CG01B2        | 232890       | 739788       | 666              | Hand sample | Pyrite in brecciated zone (post Au 1)                                      | Pyrite       | 72        | -2.00                     |
|                    |                |                   | CG01N1        | 232890       | 739788       | 666              | Hand sample | Pyrite from main quartz vein (post Au 1/pre Au 2)                          | Pyrite       | 78        | 5.30                      |
|                    |                |                   | CG01N2        | 232890       | 739788       | 666              | Hand sample | Pyrite within brecciated zone (post Au 1)                                  | Pyrite       | 80        | 5.00                      |
|                    |                |                   | CG01N1        | 232890       | 739788       | 666              | Hand sample | Arsenopyrite with pyrite from main quartz vein (post Au 1/pre Au 2)        | Arsenopyrite | Laser     | 5.40                      |
|                    |                |                   | CG01S1        | 232890       | 739788       | 666              | Hand sample | Pyrite isolated in quartz (post Au 1)                                      | Pyrite       | 99        | 4.25                      |
|                    |                |                   | CG01S2        | 232890       | 739788       | 666              | Hand sample | Pyrite next to sphalerite in main quartz vein (post Au 1)                  | Pyrite       | 83        | 4.70                      |
|                    |                |                   | CG01S1        | 232890       | 739788       | 666              | Hand sample | Chalcopyrite with pyrite in main quartz vein (post Au 1)                   | Chalcopyrite | Laser     | 5.00                      |
|                    |                |                   | CG01S1        | 232890       | 739788       | 666              | Hand sample | Sphalerite adjacent to pyrite in main quartz vein (Au 2)                   | Sphalerite   | 93        | 4.67                      |
|                    | Beinn Udlaiddh | Main vein         | 11/8 100 mark | 228298       | 733354       | 740              | Hand sample | Galena in with pyrite in main quartz vein (syn Au 1)                       | Galena       | 57        | 8.90                      |
|                    |                |                   | 11/8 100 mark | 228298       | 733354       | 740              | Hand sample | Pyrite with minor galena in main quartz vein (post-Au 1)                   | Pyrite       | 35        | 8.40                      |
|                    |                |                   | 27/7 Transect | 228293       | 733349       | 745              | Hand sample | Fine grained pyrite disseminated in brecciated zone (post Au 1)            | Pyrite       | 28        | 10.20                     |

(Continued)

**Table 1.** *S*-isotope results from mineralization, sedimentary and magmatic sulphide showings in the Tyndrum area (Continued)

|                    | Location       | Vein                      | ID number         | X coordinate | Y coordinate | Z coordinate (m) | Sample type      | Description   | Species      | Yield (%) | $\delta^{34}\text{S}$ (‰) |
|--------------------|----------------|---------------------------|-------------------|--------------|--------------|------------------|------------------|---|--------------|-----------|---------------------------|
| Gold-bearing veins | Beinn Udlaiddh | Main vein                 | BU11              | 226733       | 733972       | 380              | Hand sample      | Pyrite with minor galena from main quartz vein (post Au 1)                | Pyrite       | 45        | 9.70                      |
|                    |                |                           | BU12              | 228298       | 733354       | 748              | Hand sample      | Cubic pyrite from main brecciated quartz vein (post Au 1)                 | Pyrite       | 29        | 5.20                      |
|                    |                |                           | BU15              | 228069       | 733135       | 840              | Hand sample      | Fine-grained pyrite disseminated in brecciated zone (post Au 1)           | Pyrite       | 77        | 7.60                      |
|                    |                |                           | BU5               | 228375       | 733407       | 722              | Hand sample      | Fine-grained pyrite disseminated in brecciated zone (post Au 1)           | Pyrite       | 88        | 9.55                      |
|                    |                |                           | WP BU01A          | 228065       | 733121       | 830              | Hand sample      | Disseminated pyrite from sulphide zone in massive quartz vein (post Au 1) | Pyrite       | 76        | 8.16                      |
|                    |                |                           | WP BU02           | 227726       | 732746       | 813              | Hand sample      | Disseminated pyrite from sulphide zone in massive quartz vein (post Au 1) | Pyrite       | 93        | 5.74                      |
|                    |                |                           | WP BU05           | 228012       | 733069       | 838              | Hand sample      | Disseminated pyrite from sulphide zone in massive quartz vein (post Au 1) | Pyrite       | 75        | 5.83                      |
|                    |                |                           | WP BUNext         | 228346       | 733376       | 730              | Hand sample      | Massive pyrite from NE extension sulphide-rich zone (post Au 1)           | Pyrite       | 61        | 8.15                      |
|                    | Glen Cononish  | Bulk concentrate Eas Anie | Con bulkcon       |              |              |                  | Bulk concentrate | Bulk concentrate from Cononish  |              | N/A       | 6.68                      |
|                    |                |                           | A-min 738 m       | 228610       | 728079       | 400              | Adit sample      | Massive pyrite in main brecciated quartz vein (pre Au 1)                  | Pyrite       | 79        | -1.95                     |
|                    |                |                           | A-min end of adit | 228284       | 727753       | 400              | Adit sample      | Chalcopyrite with pyrite in main quartz vein (Au 2)                       | Chalcopyrite | 70        | 1.80                      |
|                    |                |                           | A-min end of adit | 228284       | 727753       | 400              | Adit sample      | Pyrite with chalcopyrite in main quartz vein (Au 2)                       | Pyrite       | 53        | 3.05                      |
|                    |                |                           | CN666             | 228536       | 728020       | 400              | Adit sample      | Highly brecciated zone within main vein (Au 2)                            | Galena       | 92        | 7.50                      |
|                    |                |                           | CN666             | 228536       | 728020       | 400              | Adit sample      | Highly brecciated zone within main vein (Au 2)                            | Pyrite       | 53        | 6.70                      |
|                    |                |                           | CO02              | 228632       | 728085       | 400              | Adit sample      | Massive pyrite from gold-rich section within early quartz (pre Au 1)      | Pyrite       | 88        | 1.83                      |

## NEOPROTEROZOIC S-ISOTOPES AND GOLD VEINS

|                      |        |        |     |             |   |              |     |       |
|----------------------|--------|--------|-----|-------------|---|--------------|-----|-------|
| CO03a                | 228632 | 728085 | 400 | Adit sample | Closely related chalcopyrite and galena in narrow late sulphide-rich shear in massive white quartz (Au 2) | Chalcopyrite | 80  | 8.20  |
| CO03b                | 228632 | 728085 | 400 | Adit sample | Closely related chalcopyrite and galena in narrow late sulphide-rich shear in massive white quartz (Au 2) | Galena       | 107 | 4.87  |
| CO03c                | 228632 | 728085 | 400 | Adit sample | Cubic pyrite from massive white quartz by sulphide-rich shear (pre Au 1)                                  | Pyrite       | 84  | 10.99 |
| CO05                 | 228770 | 728194 | 400 | Adit sample | Narrow late sulphide shear near cross-cutting Tyndrum Pb mine-style mineralization (pre Au 1)             | Pyrite       | 90  | 8.88  |
| CO12                 | 228671 | 728114 | 400 | Adit sample | Sphalerite from carbonate vein in wall rock (Au 2)  | Sphalerite   | 88  | 10.89 |
| CO14a                | 229086 | 728542 | 400 | Adit sample | Vein with brecciated and altered clasts and central sulphide-rich zone (pre Au 1)                         | Pyrite       | 61  | 4.71  |
| CO14b                | 229086 | 728542 | 400 | Adit sample | Vein with brecciated and altered clasts and central sulphide-rich zone (pre Au 1)                         | Pyrite       | 62  | 7.19  |
| Con 11B<br>248–249 m | 228613 | 728105 | 503 | Drill core  | Galena around fractured pyrite in brecciated vein (Au 2)  | Galena       | 226 | 7.80  |
| Con 11B<br>248–249 m | 228613 | 728105 | 503 | Drill core  | Fractured pyrite from brecciated quartz vein (pre Au 1)   | Pyrite       | 76  | 8.20  |
| Con 27<br>325–326 m  | 228524 | 728093 | 496 | Drill core  | Pyrite in quartz vein (pre Au 1)  | Pyrite       | 63  | 9.00  |
| EA01A                | 229060 | 728489 | 404 | Drill core  | High gold core sample, brecciated quartz vein with high sulphide content (Au 2)                           | Galena       | 83  | 4.00  |
| EA01B                | 229060 | 728489 | 404 | Drill core  | High gold core sample, brecciated quartz vein with high sulphide content (Au 2)                           | Pyrite       | 81  | 7.50  |

(Continued)

**Table 1.** *S*-isotope results from mineralization, sedimentary and magmatic sulphide showings in the Tyndrum area (Continued)

|                    | Location      | Vein               | ID number     | X coordinate | Y coordinate | Z coordinate (m) | Sample type | Description   | Species      | Yield (%) | $\delta^{34}\text{S}$ (‰) |
|--------------------|---------------|--------------------|---------------|--------------|--------------|------------------|-------------|---|--------------|-----------|---------------------------|
| Gold-bearing veins | Glen Cononish | Eas Anie           | EA01C         | 229060       | 728489       | 404              | Drill core  | High gold core sample, brecciated quartz vein with high sulphide content (Au 2)               | Galena       | 73        | 8.40                      |
|                    |               |                    | EA01D         | 229060       | 728489       | 404              | Drill core  | High gold core sample, brecciated quartz vein with high sulphide content (Au 2)               | Chalcopyrite | 80        | 5.00                      |
|                    |               |                    | EA02 60.4 m   | 229094       | 728454       | 405              | Drill core  | Pyrite in brecciated vein (pre Au 1)  | Pyrite       | 79        | 7.40                      |
|                    |               |                    | EA05 112.75 m | 229046       | 728485       | 405              | Drill core  | Pyrite in gold-bearing quartz vein which is cross-cut by Tyndrum Pb mine-style mineralization | Pyrite       | 81        | 9.10                      |
|                    |               |                    | EA06 75 m     | 229087       | 728511       | 405              | Drill core  | Pyrite in small quartz veins cross-cutting K-feldspar altered psammite (pre Au 1)             | Pyrite       | 83        | 3.70                      |
|                    |               | Coire Nan Sionnach | CNS05         | 228302       | 729714       | 670              | Hand sample | Pyrite from silicified sulphide-rich brecciated quartz vein (pre Au 1)                        | Pyrite       | 77        | 11.10                     |
|                    |               | Kilbridge          | Kil01         | 227819       | 730192       | 125              | Hand sample | Disseminated pyrite (pre Au 2) in brecciated quartz vein                                      | Pyrite       | 60        | 10.90                     |
|                    |               |                    | Kil02a        | 227718       | 730108       | 95               | Hand sample | Pyrite from dark sulphide-rich quartz vein (pre Au 2)   | Pyrite       | 65        | 8.50                      |
|                    |               |                    | Kil02b        | 227718       | 730108       | 95               | Hand sample | Pyrite disseminated in altered host rock at contact with quartz vein (pre Au 2)               | Pyrite       | 57        | 8.90                      |
|                    | Glen Orchy    |                    | GO02a         | 225922       | 734658       | 109              | Hand sample | Cubic pyrite from brecciated quartz vein (syn Au 1); cross-cuts GO1213                        | Pyrite       | 64        | 8.11                      |
|                    |               |                    | GO01          | 226467       | 735580       | 109              | Hand sample | Pyrite in contact with host rock at edge of vein (syn Au 1); cross-cuts GO1206                | Pyrite       | 57        | 9.40                      |
|                    |               |                    | GO02b         | 225922       | 734658       | 109              | Hand sample | Gold-bearing cubic pyrite from brecciated quartz vein (syn Au 1); cross-cuts GO1213           | Pyrite       | 90        | 8.20                      |
|                    |               |                    |               |              |              |                  |             |   |              |           |                           |
|                    |               | River Vein         | RV18          | 225118       | 733967       | 99               | Hand sample | Large galena blebs from complex brecciated quartz vein (syn Au 2); cross-cuts GO1218          | Galena       | 114       | 6.31                      |

## NEOPROTEROZOIC S-ISOTOPES AND GOLD VEINS

|                                      |               |          |                    |        |        |     |             |  |              |     |      |
|--------------------------------------|---------------|----------|--------------------|--------|--------|-----|-------------|--|--------------|-----|------|
|                                      |               |          | RV18               | 225118 | 733967 | 99  | Hand sample | Cubic pyrite in vein from complex brecciated quartz vein (syn Au 1); cross-cuts GO1213     | Pyrite       | 78  | 7.52 |
|                                      |               |          | RVNQ04<br>165 m    | 225184 | 734025 | 108 | Drill core  | Large pyrite in 20 cm wide brecciated quartz vein in gold-rich core (syn Au 1)             | Pyrite       | 93  | 7.77 |
|                                      | Sron Garbh    |          | SG04a              | 232065 | 732789 | 566 | Hand sample | Cubic pyrite from gold-bearing quartz vein (syn Au 1)                                      | Pyrite       | 100 | 6.77 |
|                                      |               |          | SG04b              | 232065 | 732789 | 566 | Hand sample | Cubic pyrite from vein contact with altered Meall Garbh Psammite (syn Au 1)                | Pyrite       | 58  | 9.39 |
|                                      |               |          | SG05               | 232005 | 732882 | 591 | Hand sample | Small pyrite from quartz vein (syn Au 1)   | Pyrite       | 84  | 7.78 |
|                                      |               |          | SG07a              | 232039 | 732771 | 570 | Hand sample | Large cubic pyrite in brecciated quartz vein (syn Au 1)                                    | Pyrite       | 82  | 7.41 |
|                                      |               |          | SG07b              | 232039 | 732771 | 570 | Hand sample | Pyrite in fine stringers in brecciated quartz vein (syn Au 1)                              | Pyrite       | 93  | 8.67 |
| Tyndrum Pb mine-style mineralization | Cononish      | Eas Anie | EA04 10.50 m b-min | 229125 | 728471 | 404 | Drill core  | Chalcopyrite with galena from vein cross-cutting main Cononish structure (post all Au min) | Chalcopyrite | 74  | 9.20 |
|                                      |               |          | EA04 10.50 m B-min | 229125 | 728471 | 404 | Drill core  | Galena with chalcopyrite from vein cross-cutting main Cononish structure (post all Au min) | Galena       | 94  | 6.60 |
| Barren veins                         | Glen Orchy    |          | RV14               | 225145 | 734087 | 99  | Hand sample | Pyrite from barren central vein (post Mo min)  | Pyrite       | 79  | 4.05 |
|                                      |               |          | RV15               | 225098 | 734072 | 100 | Hand sample | Pyrite from alteration zone (post Mo min)  | Pyrite       | 85  | 3.08 |
| Breccia bodies                       | Beinn Udlaidh |          | BU 22              | 226708 | 734198 | 335 | Hand sample | Large single galena grain in lamprophyre   | Galena       | 84  | 5.20 |
|                                      |               |          | BU 01              | 226636 | 733870 | 400 | Hand sample | Small cubic pyrite disseminated in matrix (post Au)  | Pyrite       | 41  | 1.30 |
|                                      |               |          | BU 12              | 227430 | 732664 | 765 | Hand sample | Small cubic pyrite disseminated in matrix (post Au)  | Pyrite       | 46  | 3.65 |

(Continued)



**Table 1.** *S-isotope results from mineralization, sedimentary and magmatic sulphide showings in the Tyndrum area (Continued)*

|                           | Location       | Vein       | ID number | X coordinate | Y coordinate | Z coordinate (m) | Sample type | Description  | Species     | Yield (%) | $\delta^{34}\text{S}$ (‰) |
|---------------------------|----------------|------------|-----------|--------------|--------------|------------------|-------------|--|-------------|-----------|---------------------------|
| Breccia bodies            | Beinn Udlaiddh |            | BU 22     | 226708       | 734198       | 335              | Hand sample | Small cluster of coarse euhedral pyrite grains in lamprophyre                              | Pyrite      | 69        | 3.80                      |
|                           |                |            | BU 11     | 225914       | 732806       | 480              | Hand sample | Small cubic pyrite disseminated in matrix (post Au)  | Pyrite      | 66        | 4.70                      |
|                           |                |            | BU 21     | 226591       | 735659       | 105              | Hand sample | Small cluster of coarse euhedral pyrite grains in lamprophyre                              | Pyrite      | 64        | 4.90                      |
|                           |                |            | BU 15     | 226718       | 733975       | 380              | Hand sample | Small cluster of fine amorphous pyrite grains, next to breccia-host rock contact (post Au) | Pyrite      | 62        | 5.15                      |
|                           |                |            | BU 16     | 226448       | 734047       | 358              | Hand sample | Large single pyrite grain in lamprophyre   | Pyrite      | 84        | 7.35                      |
| Molybdenite-bearing veins | Glen Orchy     | River Vein | RV01      | 225150       | 733968       | 95               | Hand sample | Molybdenite from K-feldspar alteration zone (syn-Mo)                                       | Molybdenite | 64        | 6.00                      |
|                           |                |            | RV109     | 225116       | 734032       | 97               | Hand sample | Molybdenite from K-feldspar alteration zone (syn-Mo)                                       | Molybdenite | 48        | 6.30                      |
|                           |                |            | GO1217    | 225122       | 734033       | 114              | Hand sample | Molybdenite from K-feldspar alteration zone (syn-Mo)                                       | Molybdenite | 63        | 6.60                      |
|                           |                |            | RV12      | 225138       | 733982       | 106              | Hand sample | Large cubic pyrite (post-Mo)   | Pyrite      | 67        | 1.83                      |
|                           |                |            | RV13b     | 225140       | 733998       | 104              | Hand sample | Pyrite in cross-cutting quartz vein (post-Mo)  | Pyrite      | 61        | 3.74                      |
|                           |                |            | RVNQ167   | 225184       | 734025       | 108              | Drill core  | Pyrite from molybdenite-rich core (post-Mo)  | Pyrite      | 75        | 3.99                      |
|                           |                |            | RV13a     | 225140       | 733998       | 104              | Hand sample | Pyrite from K-feldspar alteration zone (post-Mo)   | Pyrite      | 78        | 4.50                      |
|                           |                |            | RV10      | 225136       | 733988       | 105              | Hand sample | Pyrite from K-feldspar alteration zone (post-Mo)   | Pyrite      | 65        | 4.65                      |

## NEOPROTEROZOIC S-ISOTOPES AND GOLD VEINS

|                          |                          |        |        |        |     |             |  |        |       |       |
|--------------------------|--------------------------|--------|--------|--------|-----|-------------|--|--------|-------|-------|
| Metasedimentary<br>rocks | Auchtertyre              | RV021  | 225150 | 733968 | 95  | Hand sample | Pyrite disseminated in host<br>psammite (post-Mo)                                      | Pyrite | 73    | 5.00  |
|                          |                          | RV16   | 225111 | 733992 | 95  | Hand sample | Large cubic pyrite in quartz at<br>adjacent to alteration zone<br>(post-Mo)            | Pyrite | 72    | 6.09  |
|                          |                          | RV11   | 225136 | 733988 | 105 | Hand sample | Large cubic pyrite from late<br>quartz vein (post-Mo)                                  | Pyrite | 58    | 6.24  |
|                          |                          | RV16b  | 225111 | 733992 | 95  | Hand sample | Pyrite in quartz vein with<br>some K-feldspar alteration<br>(post-Mo)                  | Pyrite | 68    | 7.52  |
|                          |                          | RV01   | 225150 | 733968 | 95  | Hand sample | Pyrite from alteration band<br>within host rock (post-Mo)                              | Pyrite | 50    | 8.40  |
|                          | Auch Estate              | ATT06  | 235614 | 730236 | 248 | Hand sample | Disseminated pyrite from Ben<br>Challum Quartzite                                      | Pyrite | 53    | 8.00  |
|                          |                          | ATT01  | 235219 | 731141 | 321 | Hand sample | Disseminated pyrite from Ben<br>Lawers Schist  | Pyrite | 72    | –3.20 |
|                          |                          | LT02   | 235714 | 733589 | 524 | Hand sample | Disseminated pyrite from<br>Carn Mairg Quartzite                                       | Pyrite | 54    | 8.71  |
|                          |                          | GO1206 | 226467 | 735579 | 114 | Hand sample | Meall Garbh Psammite;<br>cross-cut by GO01 and<br>sample taken at contact<br>with vein | Pyrite | 62    | 4.78  |
|                          | Glen Orchy               | GO1218 | 225131 | 733961 | 96  | Hand sample | Meall Garbh Psammite;<br>cross-cut by RV18 and<br>sample taken at contact<br>with vein | Pyrite | 64    | 6.95  |
| Igneous                  | Sron Garbh<br>Glen Orchy | 17.04  | 232450 | 732991 | 490 | Drill core  | Meall Garbh Psammite   | Pyrite | Laser | 5.3   |
|                          |                          | GO1213 | 225921 | 734658 | 104 | Hand sample | Lamprophyre; cross-cut by<br>GO02b and sample taken<br>at contact with vein            | Pyrite | 62    | 6.76  |

---

All coordinates are relative to the British National Grid.

(Ben Lawers Schist), a stratabound horizon of uncertain origin (Carn Mairg Quartzite) and alteration haloes around cross-cutting veins (Table 2).  $\delta^{34}\text{S}$  values recorded for the Meall Garbh Psammite vary from +4.7 to +6.9‰ (Table 1), but are associated with mineralized veins and therefore may not represent the sedimentary values (see below). The Carn Mairg Quartzite in the Auch Estate has a stratabound sulphide horizon with a  $\delta^{34}\text{S}$  value of +8.0‰ and the Ben Challum mineralized SEDEX horizon at Auchtertyre, approximately 4 km east of Tyndrum, has a  $\delta^{34}\text{S}$  value of +8.7‰. The Ben Lawers Schist volcanogenic-related sulphides record a lower  $\delta^{34}\text{S}$  than seen in the other horizons of -3.2‰.

### *Relationship between veins and host rock alteration*

Host rock alteration of metasedimentary rocks extends up to 1 m from cross-cutting veins and is characterized by addition of sulphides (Fig. 8a, b) and alteration to a K-feldspar or chlorite-sericite assemblage. Lamprophyres cross-cut by gold-mineralized quartz veins show strong chlorite-sericite alteration over comparable distances and are only observed to contain sulphides in the alteration zone (Fig. 8c). In all veins  $\delta^{34}\text{S}$  values are higher than in the surrounding altered host rock (Fig. 8; Table 2), suggesting mixing in the alteration zone of high  $\delta^{34}\text{S}$  sulphur from the veins with host rock sulphur that has a lower ( $\leq +7\%$ )  $\delta^{34}\text{S}$  value. Host metasedimentary rocks and lamprophyre  $\delta^{34}\text{S}$  values measured in alteration haloes of cross-cutting veins are therefore not representative of original sedimentary or magmatic values, respectively, and instead are maximum values for these units. Vein fluids are thus indicated to be coming from a source with higher  $\delta^{34}\text{S}$ .

### *S-isotope fractionations between mineral pairs*

Pyrite and molybdenite pairs (Table 3) are not in sulphur isotope equilibrium when compared with experimental fractionation factors ( $\Delta^{34}\text{S} = 0.31$  to -0.12 over 400–600 °C; Suvorova 1974), with the pyrite in equilibrium with a fluid c. 2‰ higher if formed at similar temperatures. The fractionation between chalcopyrite and pyrite (Kajiwara & Krouse 1971) at Cononish indicates that, for the low  $\delta^{34}\text{S}$  values, chalcopyrite and pyrite are in equilibrium at  $326 \pm 89$  °C (Table 3), within the suggested temperature range of precipitation (290–350 °C; Curtis *et al.* 1993). At higher  $\delta^{34}\text{S}$  values fractionations between chalcopyrite and pyrite are large, resulting in low apparent temperatures (Kajiwara & Krouse 1971); chalcopyrite is likely to be

in equilibrium with a fluid c. 1.2–1.5‰ lighter if pyrite and chalcopyrite formed at 290–350 °C. Galena is consistently in disequilibrium (isotopic reversal with galena having higher values than the pyrite) over a temperature range of 250–500 °C or gives low temperatures (Table 3) with chalcopyrite and pyrite (Kajiwara & Krouse 1971; Li & Lui 2006). The S-isotope equilibrium fractionations between galena and chalcopyrite at Cononish give low temperatures that might reflect cooling during the development of the paragenesis. While the fractionation of S-isotope between arsenopyrite and pyrite is not constrained, the similar  $\delta^{34}\text{S}$  values observed at Coire a'Ghabalach (Table 3) suggest that equilibrium was reached (Nesbitt 1988). Overall, the S-isotope fractionations are consistent with the petrographic evidence of early pyrite and later chalcopyrite and galena.

## **Discussion**

The wide range in S-isotope values from mineralization in the Tyndrum area is inconsistent with a single source for the sulphur in these occurrences. Curtis *et al.* (1993) suggested that the sulphur in the Cononish gold-bearing quartz vein mineralization had to have derived a significant proportion from the Dalradian sedimentary succession, the remainder being of magmatic origin. Results from this study confirm that sedimentary sulphur is a significant source in the gold mineralized veins, breccia bodies and molybdenite mineralization in the Tyndrum area, and the enhanced dataset is used here to identify the likely sedimentary source rocks and their contribution to the veins, in particular whether the Grampian and lower-Appin host units could contribute to the sedimentary sulphur component. Following definition of the magmatic end-member and review of the existing data for the Dalradian metasedimentary pile, the likely sedimentary  $\delta^{34}\text{S}$  values and how they vary through the Dalradian succession are further constrained by correlating the global  $\delta^{34}\text{S}$  curve (Halverson *et al.* 2010) to the Dalradian stratigraphy. This provides probable  $\delta^{34}\text{S}$  values for sulphur-poor metasedimentary rocks that have only limited existing data.

### *Magmatic S-sources*

Sulphides in mineralization associated with plutonic intrusions across the area average  $\delta^{34}\text{S} +2.6 \pm 1.8\%$  (Fig. 4; Lowry *et al.* 1995) and, specifically, sulphides from the Etive granite (Fig. 1) have an average  $\delta^{34}\text{S}$  of +2.1‰, suggesting that the granite may have derived some sulphur from crustal sources during emplacement (Lowry *et al.* 2005).

**Table 2.** *Geochemistry and S-isotope data of host lithology and key magmatic bodies and associated cross-cutting veins in the Tyndrum area*

| Sample ID | Location    | Type        | Xco    | Yco    | Zco (m) | Lithology  | Origin of sulphides                              | S(%) | Species | $\delta^{34}\text{S}$ (‰) |
|-----------|-------------|-------------|--------|--------|---------|--|--|------|---------|---------------------------|
| ATT04     | Auchtertyre | Hand sample | 235443 | 729154 | 200     | Ben Lui Schist   | Volcanogenic                                     | 0.02 |         |                           |
| ATT06     | Auchtertyre | Hand sample | 235614 | 730236 | 248     | Ben Challum Quartzite                                      | Syn-sedimentary mineralized SEDEX horizon        | 1.27 | Pyrite  | 8.00                      |
| ATT07     | Auchtertyre | Hand sample | 235602 | 730229 | 243     | Ben Challum Quartzite                                      | Syn-sedimentary mineralized SEDEX horizon        | 2.32 |         |                           |
| ConBG10   | Cononish    | Hand sample | 231077 | 728647 | 254     | Ben Lawers Schist  | Volcanogenic                                     | 0.23 |         |                           |
| ATT01     | Auchtertyre | Hand sample | 235219 | 731141 | 321     | Ben Lawers Schist  | Volcanogenic                                     | 1.78 | Pyrite  | – 3.20                    |
| ATT02     | Auchtertyre | Hand sample | 235271 | 731056 | 317     | Ben Lawers Schist  | Volcanogenic                                     | 0.51 |         |                           |
| ConBG11   | Cononish    | Hand sample | 228987 | 727238 | 305     | Ardrihaig Phyllite   | Diagenetic sedimentary                           | 0.02 |         |                           |
| ConBG05   | Cononish    | Hand sample | 228108 | 727380 | 354     | Ben Eagach Schist with pyrite                              | Syn-sedimentary mineralized SEDEX horizon        | 0.39 |         |                           |
| ConBG06   | Cononish    | Hand sample | 228424 | 727236 | 330     | Ben Eagach Schist with pyrite                              | Syn-sedimentary mineralized SEDEX horizon        | 0.99 |         |                           |
| LT02      | Auch Estate | Hand sample | 235714 | 733589 | 524     | Carn Maig Quartzite  | Unconstrained stratabound un-mineralized horizon | 0.14 | Pyrite  | 8.71                      |
| ConBG02   | Cononish    | Hand sample | 227080 | 727700 | 420     | Carn Maig Quartzite  | Unconstrained stratabound un-mineralized horizon | 0.01 |         |                           |
| ConBG03   | Cononish    | Hand sample | 227101 | 727751 | 413     | Leven Schist   | No sulphides present                             | 0.01 |         |                           |
| GO1219    | Glen Orchy  | Hand sample | 224998 | 733606 | 95      | Beinn Udlaidh Quartzite                                    | No sulphides present                             | 0.02 |         |                           |
| GO1220    | Glen Orchy  | Hand sample | 224624 | 732702 | 82      | Beinn Udlaidh Quartzite                                    | No sulphides present                             | 0.01 |         |                           |
| BGA06     | Auch        | Hand sample | 233561 | 736344 | 223     | Meall Garbh Psammite                                       | No sulphides present                             | 0.09 |         |                           |
| GO1202    | Glen Orchy  | Hand sample | 227536 | 736730 | 124     | Meall Garbh Psammite 1 m from K-feldspar alteration        | No sulphides present                             | 0.19 |         |                           |
| GO1203    | Glen Orchy  | Hand sample | 227345 | 736570 | 122     | Meall Garbh Psammite near 0.5 m from K-feldspar alteration | No sulphides present                             | 0.01 |         |                           |
| GO1207    | Glen Orchy  | Hand sample | 226467 | 735579 | 114     | Meall Garbh Psammite 5 m from vein GO01                    | No sulphides present                             | 0.01 |         |                           |
| GO1206    | Glen Orchy  | Hand sample | 226467 | 735579 | 114     | Meall Garbh Psammite at contact with GO01                  | Vein cross-cutting                               | 0.40 | Pyrite  | 4.78                      |
| GO1216    | Glen Orchy  | Hand sample | 225106 | 734092 | 104     | Meall Garbh Psammite 2 m from RV18                         | No sulphides present                             | 0.05 |         |                           |
| GO1218    | Glen Orchy  | Hand sample | 225131 | 733961 | 96      | Meall Garbh Psammite at contact with RV18                  | Vein cross-cutting                               | 0.76 | Pyrite  | 6.95                      |
| GO1210    | Glen Orchy  | Hand sample | 225870 | 734653 | 108     | Lamprophyre sill 40 m away from veins                      | No sulphides present                             | 0.20 |         |                           |
| GO1213    | Glen Orchy  | Hand sample | 225921 | 734658 | 104     | Mineralized lamprophyre sill cut by GO02b                  | Vein cross-cutting                               | 2.26 | Pyrite  | 6.76                      |
| GO01      | Glen Orchy  | Hand sample | 226467 | 735580 | 109     | Au-bearing quartz vein, 10 cm wide                         | Sulphides within vein                            | 7.12 | Pyrite  | 9.40                      |
| RV18      | Glen Orchy  | Hand sample | 225118 | 733967 | 99      | Au-bearing quartz vein, up to 1 m wide                     | Sulphides within vein                            | 1.66 | Pyrite  | 7.52                      |
| GO02b     | Glen Orchy  | Hand sample | 225922 | 734658 | 109     | Au-bearing quartz vein, up to 30 cm wide                   | Sulphides within vein                            | 7.13 | Pyrite  | 8.2                       |

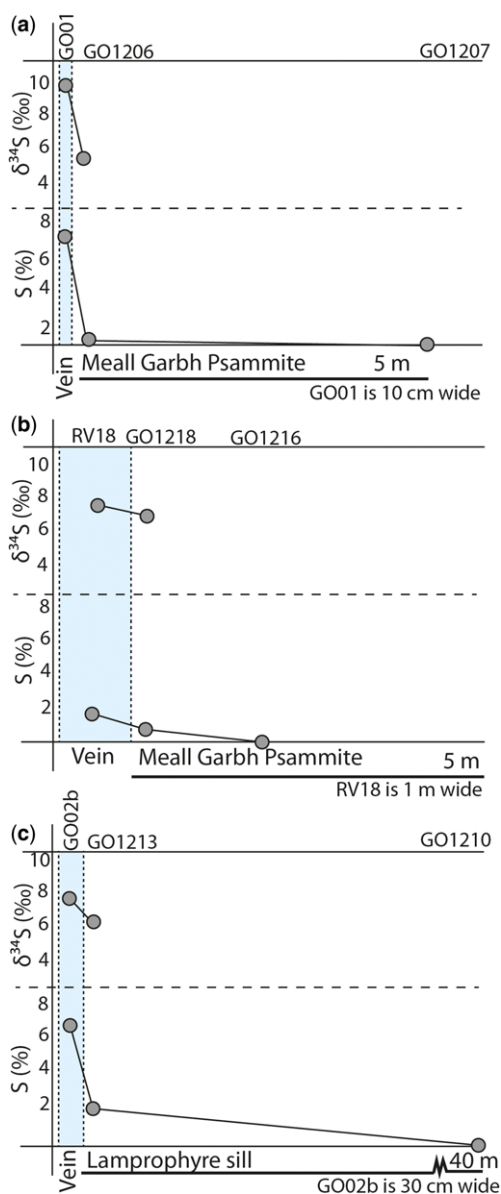


**Fig. 8.** Variation in host rock  $\delta^{34}\text{S}$  and S% with distance away from gold-bearing quartz veins: (a, b) psammite host rock; (c) Lamprophyre host rock.

$\delta^{34}\text{S}$  values from the Sron Garbh intrusion ( $\delta^{34}\text{S} = +1.0$  to  $+4.8\text{‰}$ ; Fig. 3; Fig. 7b) are comparable to apinitic pipes elsewhere in the Dalradian ( $\delta^{34}\text{S} = -2$  to  $+6\text{‰}$ ; Lowry 1991; Lowry *et al.* 1995). Thus it appears that all potential magmatic sources have  $\delta^{34}\text{S}$  values slightly higher than uncontaminated mantle-derived melts ( $\delta^{34}\text{S} = 0 \pm 3\text{‰}$ ; Ohmoto 1986).

### Sedimentary S-sources

The extensive dataset of  $\delta^{34}\text{S}_{\text{sulphide}}$  for Dalradian metasedimentary rocks (Appin–Southern Highland Groups) records large variations through the sequence (Figs 4 & 9; Willan & Coleman 1983; Scott *et al.* 1987, 1991; Hall *et al.* 1988, 1994a, b; Lowry 1991), ranging from as low as  $-15\text{‰}$  in the Ardrishaig Phyllite to as high as  $+42\text{‰}$  in Bonahaven Dolomite, consistent with the large variations in  $\delta^{34}\text{S}_{\text{sulphide}}$  in the global Neoproterozoic record ( $\delta^{34}\text{S}_{\text{sulphide}} = -30$  to  $+50\text{‰}$ ; Halverson *et al.* 2010). Sulphates have a limited occurrence in the Dalradian Supergroup and are mostly confined to the Aberfeldy deposits (Willan & Coleman 1983; Hall *et al.* 1991; Moles *et al.* 2014).

Most of the sulphide data come from the Argyll Group, with only data from the Ballachulish Slate Formation deeper in the sequence.

Stratabound sulphides in the Dalradian sequence are of three types: (a) sedimentary diagenetic sulphides which have usually undergone some recrystallization during regional metamorphism; (b) sulphide-rich but un-mineralized horizons thought to be of volcanogenic origin; and (c) syn-sedimentary mineralized hydrothermal exhalative SEDEX horizons. All three types of sulphide could be potential sources for the sulphide in the Tyndrum mineralization and all are referred to as 'sedimentary-sourced'. However, only sedimentary diagenetic sulphides that have been metamorphosed as a closed system are expected to correlate with the global sedimentary sulphide S-isotope record.

Sulphide  $\delta^{34}\text{S}$  values within the un-mineralized Ballachulish Slate (Appin Group; Fig. 2), Bonahaven Dolomite, Ben Eagach Schist and Ardrishaig Phyllite ( $\delta^{34}\text{S} = -15$  to  $+42\text{‰}$ ; Willan & Coleman 1983; Hall *et al.* 1987, 1994a, b; Lowry 1991; Moles *et al.* 2014) represent the background diagenetic sedimentary record. Diagenetic sedimentary sulphides in the Ben Eagach Schist have  $\delta^{34}\text{S}$  values in the range  $-5.7$  to  $+18\text{‰}$  (Willan & Coleman 1983; Moles *et al.* 2014). The Ardrishaig Phyllite ( $\delta^{34}\text{S} = -15$  to  $-1\text{‰}$ ; Willan & Coleman 1983; Hall *et al.* 1994a) is sulphur-poor in the Tyndrum area and Lowry *et al.* (1995) noted a lack of contamination by external sulphur in porphyries hosted in the Ardrishaig Phyllite, indicating that it is unlikely to represent a significant sulphur source. Sulphur isotopic signatures from sulphides in the Bonahaven Dolomite are not typical of diagenetic pyrite ( $\delta^{34}\text{S} = +29$  to  $+42\text{‰}$ ; Willan & Coleman 1983; Hall *et al.* 1994b; Moles *et al.* 2014) and are probably the result of closed-system reduction of evaporite sulphate (Hall *et al.* 1994b).

Sulphides within stratabound horizons of likely volcanogenic origin in the Ben Lawers and Ben



## NEOPROTEROZOIC S-ISOTOPES AND GOLD VEINS

Lui Schists, and in the Tayvallich Volcanics, have  $\delta^{34}\text{S}$  sulphide values between  $-4$  and  $+8\text{‰}$  (Willan & Coleman 1983; Scott *et al.* 1987; Lowry 1991), with a single pyrite  $\delta^{34}\text{S}$  value from this study from the Ben Lawers Schist ( $-3.2\text{‰}$ ; Fig. 7b; Table 2) being comparable. These sulphides are interpreted to be related to the appearance of mafic lavas and sills (now amphibolites) in the Dalradian sequence (Scott *et al.* 1991; Stephenson & Gould 1995).

The Aberfeldy Ba–Zn–Pb SEDEX deposits, Perthshire, are hosted largely in the Ben Eagach Schist Formation (Willan & Coleman 1983; Moles 1985; Moles *et al.* 2014). Sulphide  $\delta^{34}\text{S}$  values of the mineralization range from  $+18$  to  $+28\text{‰}$  (pyrite average  $+23.7\text{‰}$ ) and barite  $\delta^{34}\text{S}_{\text{sulphate}}$  values from  $+27$  to  $+42\text{‰}$  (average  $36 \pm 1.5\text{‰}$ ; Willan & Coleman 1983; Hall *et al.* 1987; Scott *et al.* 1991; Moles *et al.* 2014). In addition, the Ben Challum Quartzite is host to SEDEX mineralization (Fortey & Smith 1986) and a pyrite  $\delta^{34}\text{S}$  value from this study ( $\delta^{34}\text{S} = +8.0\text{‰}$ ; Fig. 7b; Table 1) is comparable to existing data ( $\delta^{34}\text{S}_{\text{sulphide}} = +8$  to  $+15\text{‰}$ ; Scott *et al.* 1987; Fig. 4).

All of the vein samples discussed in this paper are hosted in Grampian and lower-Appin Group units (Fig. 2), in particular the Meall Garbh Psammitic, Beinn Udlaidh Quartzite and Leven Schists. The units are sulphur-poor with bulk sulphur less than  $0.2\%$ , except where units are cross-cut by mineralized veins (Fig. 8; Table 2). Consistent with this, Laouar (1987) noted that no sulphide mineralization is observed in granites hosted within Grampian Group units, suggesting that the host rocks of the mineralization may not have been good sulphur sources. There are no published  $\delta^{34}\text{S}_{\text{sulphide}}$  or  $\delta^{34}\text{S}_{\text{sulphate}}$  data for these units.

To estimate the  $\delta^{34}\text{S}$  values that might occur in trace sulphides in the Grampian and lower-Appin Group stratigraphic units the global composite sulphide S-isotope curve of Halverson *et al.* (2010) is superimposed onto the Dalradian stratigraphy using two age correlations suggested by previous workers (Figs 2 & 9). In both correlations the top of the Argyll Group (Tayvallich Volcanics) is fixed at  $601 \pm 4$  Ma (Dempster *et al.* 2002). The potential correlations are:

- (1) The base of the Dalradian is *c.* 800 Ma (Noble *et al.* 1996) and, following Prave *et al.* (2009), the Port Askaig Tillite is correlated with the Sturtian glacial episodes and the mid-Easdale Subgroup is correlated to Marinoan glacial episodes.
- (2) The base of the Dalradian is *c.* 700 Ma based on  $^{87}\text{Sr}/^{86}\text{Sr}$  variation (Thomas *et al.* 2004; Stephenson *et al.* 2013); this is consistent with the Re–Os date for the Ballachulish

Slate (Rooney *et al.* 2011), which in turn suggests that the Port Askaig Tillite represents the Marinoan glacial episodes.

Comparison of the measured  $\delta^{34}\text{S}$  for the Dalradian sequence with the global curve shows a good fit for correlation 1, the only outlying points being the mineralized horizons of the Ben Eagach Schist, but given that this is a SEDEX horizon with a hydrothermal component to the sulphides (Willan & Coleman 1983; Moles *et al.* 2014), it would not be expected to fit the global curve. The good fit of the Bonahaven Dolomite data to correlation 1 may be fortuitous as this is interpreted as being a local signature owing to closed-system reduction of evaporites, not a global signal. For correlation 2 the fit is rather poorer, but this correlation is still broadly consistent with the mostly positive  $\delta^{34}\text{S}$  values measured through the Argyll Group. Further research is clearly required to refine correlations and distinguish local from global signals; nevertheless all existing data and both fits of the global curve indicate a significant amount of sedimentary and hydrothermal sulphide with positive  $\delta^{34}\text{S}$  in the Easdale Subgroup stratigraphic units. Deeper in the stratigraphy, both correlations give good fits to the Ballachulish Slate data. Below this the correlations are used to provide predictions of  $\delta^{34}\text{S}$  in the Grampian and lower-Appin host rocks. Using correlation 1 (Figs 2 & 9) the pre-Sturtian  $\delta^{34}\text{S}$  record is limited but suggests Grampian and lower-Appin Group host rocks may have an average  $\delta^{34}\text{S}$  value less than  $0\text{‰}$ , although some units could be enriched in  $^{34}\text{S}$  by up to  $10\text{‰}$ . Using correlation 2 (Figs 2 & 9), the host rocks are expected to all have  $\delta^{34}\text{S} \geq 0\text{‰}$ , with values as high as  $+40\text{‰}$  possible. This would not be consistent with observations of veins having higher  $\delta^{34}\text{S}$  than their host rocks (Fig. 8). In either case, the lack of sulphur in the local Grampian and lower-Appin Group metasedimentary rocks (Table 2) suggests that they are unlikely sources of sulphur, although they could still potentially contribute  $^{34}\text{S}$ -enriched sulphur if correlation 2 was correct.

The Islay Subgroup is not present in the Tyndrum area owing to the Boundary Slide and thus could not be the source of  $^{34}\text{S}$ -enriched sulphide in the Tyndrum mineralization. However, the Easdale Subgroup (Fig. 2) has varied  $\delta^{34}\text{S}$  values ( $\delta^{34}\text{S} = -15$  to  $+28\text{‰}$ ; Figs 4 & 9), but is largely enriched in  $^{34}\text{S}$ , in particular within the Ben Challum Quartzite and Ben Eagach Schist SEDEX horizons. In addition, these units are sulphur-rich (bulk S =  $0.39\%$  to  $2.32\%$ ; Table 2), suggesting that lithologies in this subgroup have the potential to act as a significant source of sulphur. Thus, it is proposed that the only feasible source for the sedimentary sulphur component in

**Table 3.** *S*-isotope fractionation data and calculated apparent equilibrium temperatures for mineral pairs in the Tyndrum area

|                   | Location       | Vein              | ID number         | Species      | Yield (%) | $\delta^{34}\text{S}$ (‰) | Species | $\Delta^{34}\text{S}$ (‰) | Temperature range (°C) |  |  |   |
|-------------------|----------------|-------------------|-------------------|--------------|-----------|---------------------------|---------|---------------------------|------------------------|--|--|---|
| Gold veins        | Auch Estate    | Coire a'Ghabalach | CG01S2            | Pyrite       | 83        | 4.70                      | Py–Sph  | 0.03                      |                        | Disequilibrium over temperature range 250–500 °C |  |   |
|                   |                |                   | CG01S1            | Sphalerite   | 93        | 4.67                      |         |                           |                        |  |  |   |
|                   |                |                   | CG01N1            | Pyrite       | 78        | 5.30                      |         |                           |                        |  |  |   |
|                   |                |                   | CG01N1            | Arsenopyrite | Laser     | 5.40                      |         |                           |                        |  |  |   |
|                   | Beinn Udlaiddh | Main vein         | 11/8 100 mark     | Galena       | 57        | 8.90                      |         | –0.50                     |                        | Disequilibrium over temperature range 250–500 °C |  |   |
|                   |                |                   |                   |              |           |                           |         |                           |                        |  |  |   |
|                   | Cononish       | Eas Anie          | 11/8 100 mark     | Pyrite       | 35        | 8.40                      |         |                           |                        |  | Equilibrium – realistic temperature for Cononish |   |
|                   |                |                   | A-min end of adit | Chalcopyrite | 70        | 1.80                      | Py–Cpy  | 1.25                      | 326 ± 89               |  |  |   |
|                   |                |                   | A-min end of adit | Pyrite       | 53        | 3.05                      |         |                           |                        |  |  |   |
|                   |                |                   | CN666             | Galena       | 92        | 7.50                      | Py–Gal  | –0.80                     |                        | Disequilibrium over temperature range 250–500 °C |  |   |
|                   |                |                   | CN666             | Pyrite       | 53        | 6.70                      |         |                           |                        |  |  |   |
|                   |                |                   | CO03a             | Chalcopyrite | 80        | 8.20                      | Py–Cpy  | 2.79                      | 128 ± 23               |  |  | Possibly in equilibrium but temperatures recorded are lower than previously noted at Cononish |
|                   |                |                   | CO03b             | Galena       | 107       | 4.87                      | Py–Gal  | 6.12                      | 150 ± 11               |  |  |   |
|                   |                |                   | CO03c             | Pyrite       | 84        | 10.99                     | Cpy–Gal | 3.34                      | 167 ± 22               |  |  |   |
|                   |                |                   | Con 11B 248–249 m | Galena       | 226       | 7.80                      | Py–Gal  | 0.40                      | 1385 ± 405             | Disequilibrium – unrealistic temperature         |  |   |
| Con 11B 248–249 m |                |                   | Pyrite            | 76           | 8.20      |                           |         |                           |                        |  |  |   |

|                |               |            |       |              |     |      |           |       |           |   |
|----------------|---------------|------------|-------|--------------|-----|------|-----------|-------|-----------|---|
|                |               |            | EA01A | Galena a     | 83  | 4.00 | Py–Gal a  | 3.50  | 287 ± 26  | Possibly in equilibrium   |
|                |               |            | EA01B | Pyrite       | 81  | 7.50 | Py–Gal b  | –0.90 |           | Disequilibrium over temperature range 250–500 °C  |
|                |               |            | EA01C | Galena b     | 73  | 8.40 | Py–Cpy    | 2.50  | 150 ± 29  | Possibly in equilibrium but temperatures recorded are lower than previously noted at Cononish |
|                |               |            | EA01D | Chalcopyrite | 80  | 5.00 | Cpy–Gal a | 1.00  | 523 ± 167 | Disequilibrium – unrealistic temperature  |
|                |               |            |       |              |     |      | Cpy–Gal b | –3.40 |           | Disequilibrium over temperature range 250–500 °C  |
|                | Glen Orchy    | River Vein | RV18  | Galena       | 114 | 6.31 | Py–Gal    | 1.22  | 676 ± 144 | Disequilibrium – unrealistic temperature  |
|                |               |            | RV18  | Pyrite       | 78  | 7.52 |           |       |           | Disequilibrium over temperature range 250–500 °C  |
| Breccia bodies | Beinn Udlaidh |            | BU 22 | Galena       | 84  | 5.20 | Py–Gal    | –1.40 |           | Disequilibrium over temperature range 250–500 °C  |
|                |               |            | BU 22 | Pyrite       | 69  | 3.80 |           |       |           |   |
| Molybdenite    | Glen Orchy    | River Vein | RV01  | Molybdenite  | 64  | 6.00 | Moly–Py   | –2.40 |           | Disequilibrium over temperature range 400–650 °C  |
|                |               |            | RV01  | Pyrite       | 50  | 8.40 |           |       |           |   |

Temperature range used to calculate  $\Delta^{34}\text{S}$  (‰) between mineral pairs is given in Table 4.

**Table 4.** *Temperature range over which the fractionation factor between mineral pairs is calculated*

| $\Delta^{34}\text{S}$ species | Temperature range ( $^{\circ}\text{C}$ ) | References               |
|-------------------------------|--|--------------------------|
| Py–Sph                        | 250–500                                  | Kajiwara & Krouse (1971) |
| Py–Gal                        | 250–500                                  | Kajiwara & Krouse (1971) |
| Py–Cpy                        | 250–500                                  | Kajiwara & Krouse (1971) |
| Moly–Py                       | 400–650                                  | Suvorova (1974)          |
| Cpy–Gal                       | 250–500                                  | Kajiwara & Krouse (1971) |
| Gal–Cpy                       | 250–500                                  | Li & Lui (2006)          |

the Tyndrum mineralization is the Easdale Subgroup, stratigraphically above the mineralization. Taken at face value, this could be interpreted to suggest that fluids carrying sulphur, and possibly gold and other metals, are moving down through the stratigraphy.

#### *Input of sedimentary v. magmatic sulphur into mineralized veins and breccia bodies*

It is possible to account for the total range of vein  $\delta^{34}\text{S}$  values observed in this study ( $\delta^{34}\text{S} = -2$  to  $+12\text{‰}$ ; Fig. 7) with various mixtures of sulphides from the Easdale Subgroup units ( $\delta^{34}\text{S} = -4$  to  $+22\text{‰}$ ; Figs 4 & 9) and there is no requirement to invoke an magmatic component, even for vein sulphide  $\delta^{34}\text{S}$  values close to  $0\text{‰}$  (cf. *Craw et al.* (1995) noted  $\delta^{34}\text{S}_{\text{sulphide}}$  values of  $-3$  to  $-1\text{‰}$  for the metamorphogenic Macraes gold mineralization). However, given the likely age and late tectonic setting, together with the wide range in

$\delta^{34}\text{S}$  observed in the Tyndrum area mineralization, variable mixing of magmatic and sedimentary sulphur is assumed here and the possible sedimentary rock-sourced end-members that would have been available, including both diagenetic and syn-sedimentary hydrothermal sources, are examined in Figure 10. Apart from five outliers out of 60 measurements, gold veins generally have  $\delta^{34}\text{S}$  values in the range  $+3$  to  $+12\text{‰}$ . Veins with  $\delta^{34}\text{S}$  values of  $+12\text{‰}$  can only be formed with 32–66% sulphur sourced from the SEDEX Ben Eagach horizon, 62–100% of the most  $^{34}\text{S}$ -rich diagenetic values from the Ben Eagach Schist, or 71–100% sedimentary sulphur sourced from the Ben Challum horizon (Fig. 10). It is not possible to generate a  $\delta^{34}\text{S}$  of  $+12\text{‰}$  by mixing involving sulphur from any other part of the stratigraphy in the area. Thus the highest  $\delta^{34}\text{S}$  values measured in the veins place very strong constraints on the sources of sulphur and the hydrothermal pathways in the mineralizing system, with a magmatic

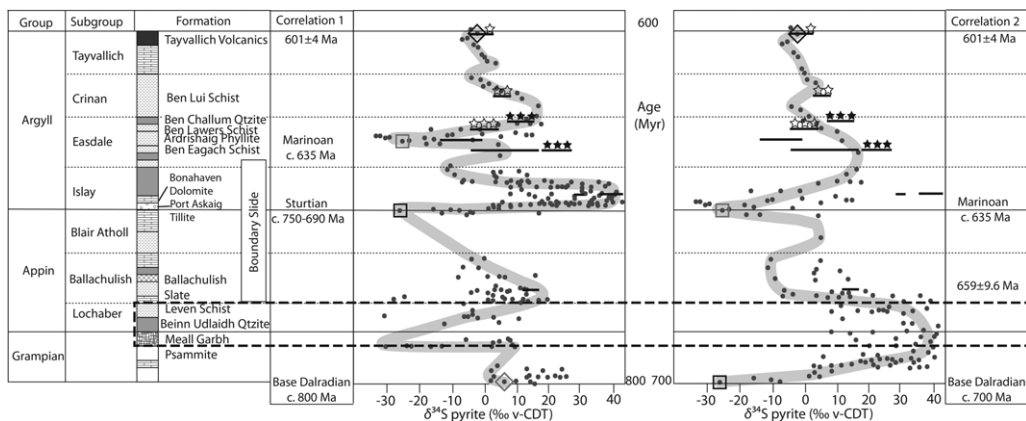


**Fig. 9.** The global composite sulphide S-isotope curve of Halverson *et al.* (2010) superimposed onto the Dalradian stratigraphy using the two correlations detailed in Figure 2. The global data (grey dots; grey zone = line of best fit) are interpolated between tie points detailed in the text (black square and diamond; grey square and diamond) by simply scaling to stratigraphic thickness (Stephenson & Gould 1995; Stephenson *et al.* 2013). Solid black lines show the existing  $\delta^{34}\text{S}_{\text{sulphide}}$  data for the Dalradian sedimentary succession (Fig. 4); open stars indicate volcanogenic sulphide horizons; black dashed box indicates host stratigraphy of mineralization in the Tyndrum area.

## NEOPROTEROZOIC S-ISOTOPES AND GOLD VEINS

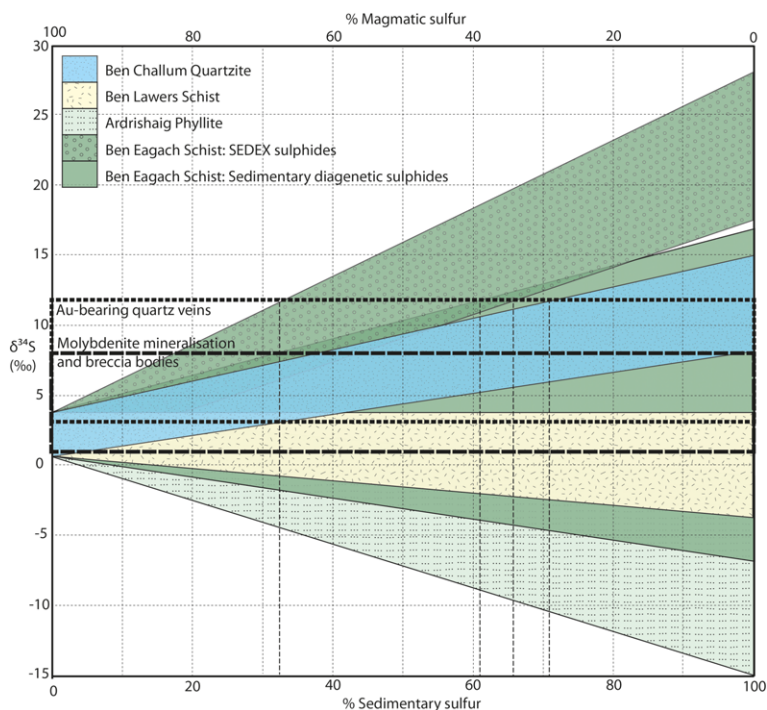


**Fig. 10.** Mixing diagram showing percentage of sulphur from a magmatic and various possible sedimentary components required to account for the observed  $\delta^{34}\text{S}$  mineral values. Vertical lines demonstrate the example of a mixture with  $\delta^{34}\text{S} = +12\text{‰}$  that could be formed by mixing of magmatic sulphur with 33–66% sedimentary sulphide from the Ben Eagach SEDEX horizon, 66–100% from diagenetic sulphides from the Ben Eagach Schist or 71–100% from the Ben Challum horizon. References as given in Figure 4. Typical ranges of  $\delta^{34}\text{S}$  mineral values are shown for gold-bearing quartz veins, and for molybdenite mineralization and breccia bodies. Magmatic values are average  $\delta^{34}\text{S}$  values from plutons in the Dalradian Supergroup ( $\delta^{34}\text{S} = +2.6 \pm 1.8\text{‰}$ ; Lowry *et al.* 1995).

sulphur input constrained to a maximum of 68%. As vein  $\delta^{34}\text{S}$  values decrease, it becomes possible to invoke mixtures involving other sedimentary units, and sulphides in gold-bearing quartz veins with  $\delta^{34}\text{S}$  values of  $+3\text{‰}$  could be 100% sourced from a magmatic component, or 100% from the Ben Lawers Schist or sedimentary diagenetic sulphides in the Ben Eagach Schist (Fig. 10). However, for vein values of  $+3\text{‰}$ , maximum proportions of sulphur from the syn-sedimentary SEDEX Ben Eagach Schist and Ben Challum Quartzite horizons are constrained to be  $<14$  and  $<32\%$  respectively.

The breccia bodies and molybdenite mineralization have similar  $\delta^{34}\text{S}$  ranges ( $+1$  to  $+8\text{‰}$ ; Fig. 10). The high  $\delta^{34}\text{S}$  values for the molybdenite mineralization compared with data from the regional magmatic complexes (Lowry *et al.* 1995; Conliffe *et al.* 2009) suggest a larger component of sedimentary-derived sulphur in the molybdenite mineralization in the Glen Orchy area. Breccia bodies or molybdenite mineralization with  $\delta^{34}\text{S}$  values of  $+8\text{‰}$  could have 18–43% sedimentary

sulphur, sourced from the syn-sedimentary SEDEX Ben Eagach horizon or 37–100% sedimentary sulphur sourced from the Ben Challum horizon. If it is assumed that the sulphur in all the mineralization was derived from the same sedimentary-sourced end-member, sulphur isotope values indicate that the molybdenite mineralization and gold-bearing mineralized breccia pipes have a larger magmatic component than gold-bearing quartz veins.

### Implications of structure

The S-isotope data suggest that a significant component of the sulphur in the Tyndrum veins is sourced from the Easdale Subgroup, higher in the stratigraphy. The Eas Anie structure, host to Cononish gold mineralization (Fig. 3), is not observed to cut the Boundary Slide at the current topography but is postulated to have extended across the Slide at emplacement, approximately 200 m above the mine portal (Tanner 2012). Thus here it might be possible that sulphides from the Easdale Subgroup could have been dissolved and re-precipitated in



the mineralization. However, at Glen Orchy and Beinn Udlaidh, the Easdale Subgroup and higher stratigraphic units are estimated to be approximately 4 km above at the time of mineralization. If fluids were transported downwards from an enriched  $\delta^{34}\text{S}$  source in Easdale Subgroup rocks, it might be expected that the Cononish gold mineralization would show a greater signature of this, but  $\delta^{34}\text{S}$  values at Glen Orchy are comparable to Cononish (Fig. 7a; Table 1). In addition, the presence of hydraulic breccia bodies and quartz-breccia veins formed from supra-lithostatic fluids (Tanner 2012) suggests a fluid pressure gradient that would preclude fluids flowing downwards during breccia formation. Furthermore, it is difficult to envisage a thermochemical gradient that could transport sulphide 4 km downwards. These considerations suggest that it was unlikely that the sulphur was derived from the overlying Easdale units.

However, consideration of the fold structures of the Tyndrum area (Tanner & Thomas 2009) has implications for possible fluid-flow pathways since all interpretations suggest that Easdale Subgroup units are likely to be repeated at depth owing to the major recumbent fold of the Beinn Chuirn Anticline (Fig. 11). The details of the likely depth at which repetition might occur depend upon the interpretation of the Boundary Slide, which represents a section of missing stratigraphy in the Tyndrum area (Figs 2 & 3). Two interpretations are proposed (Fig. 11).

- (1) The Boundary Slide is a tectonic slide (Bailey 1922, Hutton 1979) that formed syn- to post-D2 (Roberts & Treagus 1979). The stratigraphy was folded around the Beinn Chuirn Anticline during D2, then removed by movement along the slide (Fig. 11a). The slide is inferred to continue to depth; the Ballachulish, Blair Atholl and Islay Subgroups and overlying stratigraphy (Fig. 2) are all interpreted to be represented on the inverted limb of the Beinn Chuirn anticline.
- (2) A more recent interpretation (Tanner & Thomas 2009) is that the Boundary Slide is a pre-tectonic disconformity, and owing to D2 folding, stratigraphic units above the slide are expected to be represented at depth beneath the Glen Orchy dome (Fig. 11b; Tanner & Thomas 2009), with the Easdale Subgroup present, but at shallower depth than in Figure 11a.

Importantly, both interpretations imply the potential presence of the Easdale Subgroup, enriched in  $^{34}\text{S}$ , at depth and would allow the sedimentary S-isotope signature associated with mineralization to instead be sourced from the overturned limb of the Beinn Chuirn Anticline *beneath* the Grampian

and lower-Appin Group rocks observed at surface. This seems a more realistic scenario and allows hotter fluids from depth (perhaps expelled by late-tectonic magmatism) to carry sulphur (and metals) upwards and along major structures into the current host rocks where precipitation is most likely driven by pressure reduction from lithostatic to hydrostatic and wall rock sulphidation. In this scenario gold-bearing quartz veins in Glen Orchy and Beinn Udlaidh would be closer to the postulated source rocks, suggesting that they should contain a greater component of sedimentary-sourced sulphur than Cononish. However, the similar  $\delta^{34}\text{S}$  values in both areas do not support this. It is proposed, that the Tyndrum fault is a key fluid pathway in Glen Cononish, allowing gold mineralization in the Eas Anie structure to source significant sedimentary sulphur (as well as magmatic sulphur) from depth despite being further above the postulated sedimentary sulphur source rocks.

### *Metal source rocks*

The S-isotope data cannot confirm, nor exclude, a magmatic input to the mineralization, although the spread of data down to approximately 0‰ could be interpreted as supporting evidence and, together with the likely age that correlates with the intrusion of the granites, suggests it is probable. Thus a magmatic source for the gold and other metals is possible. However, it is proposed that a significant proportion of the sulphur in the mineralization must have originated from Easdale Subgroup lithologies at depth, in particular the SEDEX Ben Challum or Ben Eagach horizons. While there is no requirement that metals and sulphur are derived from the same source, and this is frequently not the case in hydrothermal gold systems (Goldfarb *et al.* 1991, 2001), the S-isotope data demonstrate that mineralizing fluids originated from, or passed through, these units and hence it is reasonable to consider whether they could also be potential metal sources. This suggestion has some credence since, along with base metals, gold is known to be concentrated in shale-hosted SEDEX mineralization (e.g. Cooke *et al.* 2000; Alchin & Moore 2005). Furthermore, Willan (1996) demonstrated that the Ben Eagach Schist is regionally enriched by hydrothermal activity in Bi, Sb, As, Mo, Ni and Ba, while in the section between the Tyndrum Fault and the Erich-Laidon Fault to the NW containing the study area, this unit has elevated Mo, Sb and Bi and isolated occurrences of strongly anomalous Cu, Zn and Pb. Unfortunately gold was not analysed in this study and no gold grains have been observed to date in the Aberfeldy deposits (N. Moles pers. comm.), but nevertheless it seems that SEDEX horizons in the Ben Eagach Schist represent feasible

## NEOPROTEROZOIC S-ISOTOPES AND GOLD VEINS

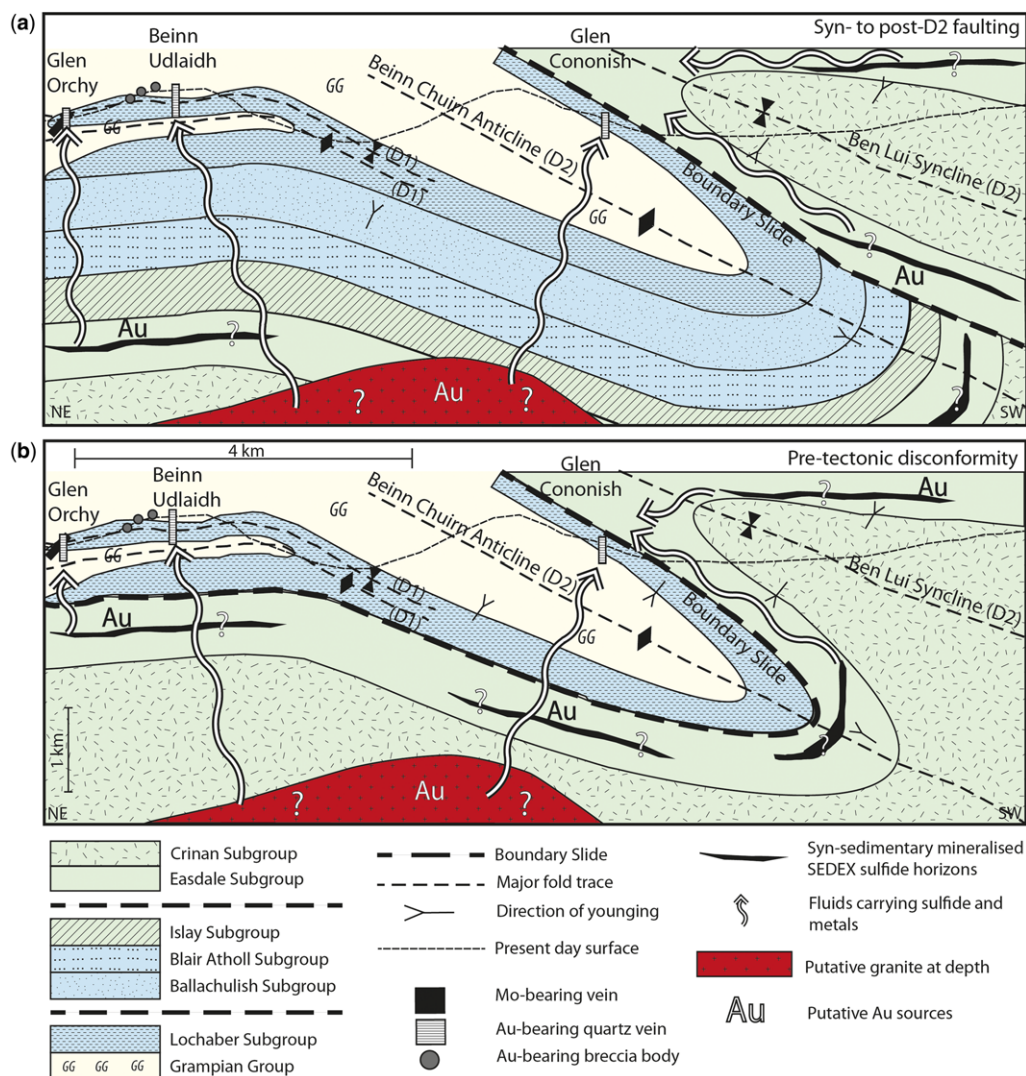


**Fig. 11.** Cross-sections through the Tyndrum area. Sulphur is interpreted to be sourced from stratigraphic units enriched in  $^{34}\text{S}$  at depth, dependent upon the interpretation of the Boundary Slide: (a) interpretation after Roberts & Treagus (1979), the Boundary Slide is a tectonic slide formed syn- to post-D2; (b) interpretation after recent mapping at Cononish (Tanner & Thomas 2009). Diagram after Tanner & Thomas (2009). The Tyndrum Fault and many of the major structures in the area run sub-parallel to the strike of the section and much of the fluid flow is therefore likely to be parallel to the plane of the section. Vertical scale approximate only.

sources for at least some or all of the base metals in the veins, in particular lead, which is notably enriched as abundant galena.

Alternatively, gold and other metals could have been pre-concentrated from the sedimentary–volcanic pile during formation of volcanogenic exhalative horizons, such as in the Ben Lawers Schist, which could subsequently produce gold-rich fluids (e.g. Hodgson *et al.* 1993; Mernagh &

Bierlien 2008). Some support for this comes from the observation by Moles (1985) of a gold inclusion within chalcocite–bornite in a sample of the Ben Lawers Schist.

A third option could be that the gold and other metals are sourced from carbonaceous pyritic metasedimentary rocks in the Dalradian, such as parts of the Ben Eagach Schist, since these may also concentrate gold along with other metals

including Ag, Zn, Mo and Cu (Large *et al.* 2011), as postulated for Dalradian rocks by Plant *et al.* (1997). Pitcairn *et al.* (2006) show that even quartzofeldspathic turbiditic metasedimentary rocks, which may not have anomalous metal contents, have the potential to release elements including Au, Ag, As, Sb, Hg, Mo and W during metamorphism. Tomkins (2012) argues that pyritic organic-rich sedimentary rocks deposited after the second Great Oxidation Event (635–510 Ma) have the potential to be a better source of gold (and molybdenum) than sedimentary rocks deposited earlier, owing to the increase in gold solubility in a more oxidized ocean. In both correlations (Fig. 9) sections of the Dalradian stratigraphy are deposited after 635 Ma (Marinoan) and therefore may have been enriched in gold and molybdenum at deposition.

From the discussion above it is clear that carbonaceous pyritic metasedimentary rocks could have been a potential source for the molybdenum in the earliest veins in the area. Compared with the later gold-mineralization, the generally lower  $\delta^{34}\text{S}$  value of the molybdenite mineralization indicates either that a larger proportion of magmatic sulphur, or that the sulphur is from a distinct metasedimentary source. For example, average  $\delta^{34}\text{S}$  for diagenetic sulphides in the Ben Eagach Schist is +5.6‰ (Willan & Coleman 1983; Moles *et al.* 2014), very close to the average value measured for the sulphides in the molybdenite mineralization (Fig. 7b). Thus it is possible that both the sulphur and the molybdenum in the early molybdenite mineralization could be wholly derived from parts of the Ben Eagach Schist. A potentially different source of sulphur and metals (and by inference fluid pathway) is conceivable for this mineralization given the distinct timing and nature of this mineralization compared with the later gold mineralization.

Overall there are a number of reasons why the Easdale Subgroup rocks represent the likely source of sulphur and potentially gold and other associated metals in the gold veins and thus place important constraints on the fluid pathways to the mineralized systems. Further work is required to confirm the source of gold and other metals but the presence of Easdale Subgroup units at depth may be an important criterion determining the prospectivity of the Dalradian Supergroup as a whole.

## Conclusions

This work provides clear evidence that gold and other metal mineralization hosted in the Tyndrum area, Scotland, has a mixed magmatic and sedimentary source of sulphur. The identification of the individual units in the Dalradian Supergroup that have

the potential to be the main source of sedimentary sulphur has been possible through thorough sampling of mineralization and host rock Dalradian units, and correlation with the global Neoproterozoic S-isotope record for the units that are poorly exposed or there is a lack of data for. Key conclusions can be summarized as:

- (1) The  $\delta^{34}\text{S}$  values for quartz vein-hosted gold mineralization in the Tyndrum area are variable ( $\delta^{34}\text{S} = -2$  to  $+12\text{‰}$ ), suggesting mixing between a contemporaneous magmatic sulphur component and sedimentary-sourced sulphur component derived from the Dalradian metasedimentary pile. However, a solely metasedimentary origin cannot be excluded by the data. This study concludes that the sedimentary sulphur component is not sourced from the S-poor Grampian and lower-Appin Group host rocks and the only feasible source of sedimentary sulphur in mineralization is the Easdale Subgroup, lying higher in the stratigraphy.
- (2) The Ben Eagach Schist Formation is considered to be the dominant source of the sedimentary sulphur. Gold-bearing quartz veins with  $\delta^{34}\text{S} = +12\text{‰}$  must have their sedimentary sulphur component sourced from 32–66% from lithologies similar to the Ben Eagach SEDEX horizon, 62–100% from the most  $^{34}\text{S}$  enriched diagenetic sedimentary sulphides in the Ben Eagach Schist, or 71–100% from lithologies similar to the Ben Challum SEDEX horizon. It is *not* possible to generate a  $\delta^{34}\text{S}$  of  $+12\text{‰}$  by mixing involving sulphur from any other part of the stratigraphy.
- (3) Gold-bearing breccia pipes and early molybdenite mineralization have a lower range of  $\delta^{34}\text{S}$  values ( $+1$ – $+8\text{‰}$ ) than the later gold veins and this either reflects a larger magmatic component, or derivation of sedimentary sulphur from a different part of the stratigraphy.
- (4) Easdale Subgroup units are interpreted to occur at depth beneath the lower Dalradian units observed at surface owing to repetition on the overturned limb of the recumbent Beinn Chuirn Anticline; the likely depth is dependent upon interpretation of the Boundary Slide. This allows fluids carrying sedimentary sulphur enriched in  $^{34}\text{S}$  to have been derived from depth.
- (5) The Easdale Subgroup may be enriched in gold and other metals in either SEDEX or volcanogenic exhalative horizons, or in carbonaceous sedimentary units, and therefore could have been a significant source of sulphur, gold and other metals. Magmatic fluids may still be important for transporting sulphur,

## NEOPROTEROZOIC S-ISOTOPES AND GOLD VEINS

gold and other metals and variable proportions of a magmatic sulphur component can be invoked to account for the wide range in  $\delta^{34}\text{S}$  observed.

- (6) The presence of  $^{34}\text{S}$ -enriched Easdale Sub-group lithologies containing metals and sulphur at depth may be important for forming mineralization in areas of sulphur-poor host rocks and should be potentially considered as an exploration criterion in the Dalradian Supergroup.

Nyree Hill is funded by the Natural Environment Research Council (NERC) through an Open CASE studentship NE/H017755/1 in conjunction with Scotgold Resources Ltd. Scotgold are acknowledged for their continuing financial and logistical field support and for access to company information. S-Isotope analyses were carried out at SUERC under NERC Isotope Facilities grant IP-1317-0512. A. Boyce is funded by NERC support of the Isotope Community Support Facility at East Kilbride, Scotland. S. Graham, K. Matthews, P. Moore, W. Plewes and C. Spence-Jones are acknowledged and thanked for their contribution in the field, data collection and sample preparation. G. Tanner, R. Willan, R. Chapman, D. Lowry and D. Craw are thanked for constructive discussion on the evolution of the Dalradian Supergroup and comments on an earlier version of the manuscript. The manuscript benefitted from the suggestions for improvement from N. Moles and M. Smith, who are thanked for their positive and constructive reviews, and P. Lusty is thanked for his editorial assistance.

## References

- ALCHIN, D. J. & MOORE, J. M. 2005. A review of the Pan-African, Neoproterozoic Rosh Pinah Zn–Pb deposit, southwestern Namibia. *South African Journal of Geology*, **108**, 71–86.
- ANDERTON, R. 1985. Sedimentation and Tectonics in the Scottish Dalradian. *Scottish Journal of Geology*, **21**, 407–436.
- BAILEY, E. B. 1922. The structure of the South-West Highlands of Scotland. *Quarterly Journal of the Geological Society*, **78**, 82–131.
- BAILEY, E. B. & MACGREGOR, M. 1912. The Glen Orchy Anticline (Argyllshire). *Quarterly Journal of the Geological Society*, **68**, 164–179.
- BAXTER, E. F., AGUE, J. J. & DEPAOLO, D. J. 2002. Prograde temperature–time evolution in the Barrovian-type locality constrained by Sm/Nd garnet ages from Glen Clova, Scotland. *Journal of the Geological Society, London*, **159**, 71–82.
- BIRD, A. F., THIRLWALL, M. F., STRACHAN, R. A. & MANNING, C. J. 2013. Lu–Hf and Sm–Nd dating of metamorphic garnet: evidence for multiple accretion events during the Caledonian Orogeny in Scotland. *Journal of the Geological Society, London*, **170**, 301–317.
- CAWOOD, P. A., MCAUSLAND, P. J. A. & DUNNING, G. R. 2001. Opening Iapetus: constraints from the Laurentian margin in Newfoundland. *Geological Society of America Bulletin*, **113**, 443–453.
- CONDON, D. J. & BOWRING, S. A. 2011. Chapter 9 A user's guide to Neoproterozoic geochronology. In: ARNAUD, E., HALVERSON, G. P. & SHIELDS-ZHOU, G. (eds) *The Geological Record of Neoproterozoic Glaciations*. Geological Society, London, Memoirs, **36**, 135–149.
- CONLIFFE, J., WILTON, D. H. C., FEELY, M., LYNCH, E. P. & SELBY, D. 2009. S-isotope analyses of molybdenite in the Appalachian–Caledonian Orogen, Northeastern section – 44th annual meeting. Geological Society of America, Boulder, CO, Abstracts with Programs, **41**, 81.
- CONLIFFE, J., SELBY, D., PORTER, S. J. & FEELY, M. 2010. Re–Os molybdenite dates from the Ballachulish and Kilmelford Igneous complexes (Scottish Highlands): age constraints for late Caledonian magmatism. *Journal of the Geological Society, London*, **167**, 297–302.
- COOKE, D. R., BULL, S. W., LARGE, R. R. & MCGOLDRICK, P. J. 2000. The importance of oxidised brines for the formation of Australian Proterozoic stratiform sediment-hosted Pb–Zn (Sedex) deposits. *Economic Geology*, **95**, 1–18.
- COWIE, J. W., RUSHTON, A. W. A. & STUBBLEFIELD, C. J. 1972. *A correlation of the Cambrian rocks in the British Isles*. Geological Society, London, Special Reports, **2**.
- CRANE, A., GOODMAN, S., KRABBENDAM, M., LESLIE, A. G. & ROBERTSON, S. 2002. *Geology of Sheet 56W and adjacent areas (Scotland)*. British Geological Survey, Memoirs, HMSO, London.
- CRAW, D., HALL, A. J., FALICK, A. E. & BOYCE, A. J. 1995. Sulphur isotopes in a metamorphogenic gold deposit, Macraes mine, Otago Schist, New Zealand. *New Zealand Journal of Geology and Geophysics*, **38**, 131–136.
- CURTIS, S. F., PATTRICK, R. A. D., JENKIN, G. R. T., FALICK, A. E., BOYCE, A. J. & TREAGUS, J. E. 1993. Fluid inclusion and stable isotope study of fault related mineralisation in Tyndrum area, Scotland. *Transactions of the Institute of Mining and Metallurgy (Section B: Applied Earth Science)*, **102**, 39–47.
- DALRADIAN RESOURCES INC 2012. *A Preliminary Economic Assessment of the Curraghinalt Gold Deposit, Tyrone Project, Northern Ireland*. Micon International Limited, Toronto.
- DEMPSTER, T. J., ROGERS, G. ET AL. 2002. Timing of deposition, orogenesis and glaciation within the Dalradian rocks of Scotland: constraints from U–Pb zircon ages. *Journal of the Geological Society, London*, **159**, 83–94.
- EARLS, G., PARKER, R. T. G., CLIFFORD, J. A. & MELDRUM, A. H. 1992. The geology of the Cononish gold-silver deposit, Grampian Highlands of Scotland. In: *Irish Minerals Industry 1980–1990*. Irish Association for Economic Geology, Dublin, 89–103.
- FETTES, D. J., LONG, C. B., MAX, M. D. & YARDLEY, B. W. D. 1985. Grade and time of metamorphism in the Caledonide Orogen of Britain and Ireland. In: HARRIS, A. L. (ed.) *The Nature and Timing of Orogenic Activity in the Caledonian rocks of the British Isles*. Geological Society, London, Memoirs, **9**, 41–53.



- FORTEY, N. J. & SMITH, C. G. 1986. Stratabound mineralisation in Dalradian rocks, near Tyndrum, Perthshire. *Scottish Journal of Geology*, **22**, 377–393.
- GALANTAS GOLD CORPORATION 2013. Technical Report on the Omagh Gold Project, County Tyrone, Northern Ireland. AIM announcement, 23 July 2013.
- GOLDFARB, R. J., NEWBERRY, R. J., PICKTHORN, W. J. & GENT, C. A. 1991. Oxygen, Hydrogen and Sulfur isotope studies in the Juneau Gold Belt, Southeastern Alaska: Constraints on the origin of hydrothermal fluids. *Economic Geology*, **86**, 66–80.
- GOLDFARB, R. J., GROVES, D. I. & GARDOLL, S. 2001. Orogenic gold and geologic time: a global synthesis. *Ore Geology Reviews*, **18**, 1–75.
- GOLDFARB, R. J., BAKER, T., DUBÉ, B., GROVES, D. I., HART, C. J. R. & GOSSELIN, P. 2005. Distribution, character and genesis of Au deposits in metamorphic terranes. In: HEDENQUIST, J. W., THOMPSON, J. F. H., GOLDFARB, R. J. & RICHARDS, J. P. (eds) *Economic Geology*, 100th Anniversary volume 1905–2005, **100**, 407–450.
- GORJAN, P., VEEVERS, J. J. & WALTER, M. R. 2000. Neoproterozoic S-isotope variation in Australia and global implications. *Precambrian Research*, **100**, 151–179.
- GRAHAM, S. D. 2013. *Characterisation of the newly discovered Cu-Ni-PGE mineralisation at Sron Garbh, Stirlingshire, Scotland*. Unpublished MGeol project, University of Leicester.
- GRAHAM, C. M., SKELTON, A. D. L., BICKLE, M. & COLE, C. 1997. Lithological, structural and deformational controls on fluid-flow during regional metamorphism. In: HOLNESS, M. B. (ed.) *Deformation-enhanced Fluid Transport in the Earth's Crust and Mantle*. Mineralogical Society Series, **8**. Chapman and Hall, London, 196–226.
- HALL, A. J., BOYCE, A. J. & FALICK, A. E. 1987. Iron sulphides in metasediments: isotopic support for a retrogressive pyrrhotite to pyrite reaction. *Chemical Geology (Isotope Geoscience Section)*, **65**, 305–310.
- HALL, A. J., BOYCE, A. J. & FALICK, A. E. 1988. A S-isotope study of iron sulfides in the Late Precambrian Dalradian Easdale Slate Formation, Argyll, Scotland. *Mineralogical Magazine*, **52**, 483–490.
- HALL, A. J., BOYCE, A. J., FALICK, A. E. & HAMILTON, P. J. 1991. Isotopic evidence of the depositional environment of the Late Proterozoic stratiform mineralisation Aberfeldy, Scotland. *Chemical Geology (Isotope Geoscience Section)*, **87**, 99–114.
- HALL, A. J., BOYCE, A. J. & FALICK, A. E. 1994a. A S-isotope study of iron sulfides in the Late Precambrian Dalradian Ardrishaig Phyllite Formation, Knapdale, Argyll. *Scottish Journal of Geology*, **30**, 63–71.
- HALL, A. J., MCCONVILLE, P., BOYCE, A. J. & FALICK, A. E. 1994b. Sulfides with high  $\delta^{34}\text{S}$  from the Late Precambrian Bonahaven Dolomite, Argyll, Scotland. *Mineralogical Magazine*, **58**, 486–490.
- HALLIDAY, L. B. 1962. *Report of surveys at Tyndrum*. File. British Geological Survey, Edinburgh.
- HALVERSON, G. P. & HURTGEN, M. T. 2007. Ediacaran growth of the marine sulfate reservoir. *Earth and Planetary Science Letters*, **263**, 32–44.
- HALVERSON, G. P. & SHIELDS-ZHOU, G. 2011. Chapter 4 Chemostratigraphy and the Neoproterozoic glaciations. In: ARNAUD, E., HALVERSON, G. P. & SHIELDS-ZHOU, G. (eds) *The Geological Record of Neoproterozoic glaciations*. Geological Society, London, Memoirs, **36**, 51–66.
- HALVERSON, G. P., HOFFMAN, P. F., SCHRAG, D. P., MALOOF, A. C. & RICE, A. H. 2005. Towards a Neoproterozoic composite carbon-isotope record. *Geological Society of America Bulletin*, **117**, 1181–1207.
- HALVERSON, G. P., DUDAS, F. O., MALOOF, A. C. & BOWRING, S. A. 2007a. Evolution of the  $^{87}\text{Sr}/^{86}\text{Sr}$  composition of Neoproterozoic seawater. *Palaeogeography, Palaeoclimatology, Palaeoecology*, **256**, 103–129.
- HALVERSON, G. P., MALOOF, A. C., SCHRAG, D. P., DUDAS, F. O. & HURTGEN, M. T. 2007b. Stratigraphy and geochemistry of a c. 800 Ma negative isotope interval in northeastern Svalbard. *Chemical Geology*, **237**, 23–45.
- HALVERSON, G. P., WADE, B. P., HURTGEN, M. T. & BAROVICH, K. M. 2010. Neoproterozoic chemostratigraphy. *Precambrian Research*, **182**, 337–350.
- HAMBREY, M. J. & HARLAND, W. B. (eds) 1981. *Earth's Pre-Pleistocene Glacial Record*. Cambridge Earth Science Series. Cambridge University Press, Cambridge.
- HARRIS, A. L., BALDWIN, C. T., BRADBURY, H. J., JOHNSON, H. D. & SMITH, R. A. 1978. Ensialic basin sedimentation: the Dalradian Supergroup. In: BOWES, D. R. & LEAKE, B. L. (eds) *Crustal Evolution in North-western Britain and Adjacent Regions*. Seel House Press, Liverpool, 115–138.
- HARTE, B. 1988. Lower Palaeozoic metamorphism in the Moine-Dalradian belt of the British Isles. In: HARRIS, A. L. & FETTES, D. J. (eds) *The Caledonian–Appalachian Orogen*. Geological Society, London, Special Publications, **38**, 123–134.
- HILL, A. C. & WALTER, M. R. 2000. Mid-Neoproterozoic (830–750 Ma) isotope stratigraphy of Australia and global correlation. *Precambrian Research*, **100**, 181–211.
- HILL, N. J., JENKIN, G. R. T. *ET AL.* 2011. New gold occurrences in the Scottish Dalradian – nature and constraints on genesis. In: BARRA, F., REICH, M., CAMPOS, E. & TORNOS, F. (eds) *Let's Talk Ore Deposits. Proceedings of the 11th Biennial Meeting*, Antofagasta, Chile, **2**, 577–579.
- HODGSON, C. J., LOVE, D. A. & HAMILTON, J. V. 1993. Giant mesothermal gold deposits: descriptive characteristics, genetic model and exploration area selection criteria. In: WHITING, B. H., HODGSON, C. J. & MASON, R. (eds) *Giant Ore Deposits*. Society of Economic Geologists, Littleton, CO, Special Publications, **2**, 157–212.
- HOFFMAN, P. F., KAUFMAN, A. J., HALVERSON, G. P. & SCHRAG, D. P. 1998. A Neoproterozoic Snowball Earth. *Science*, **281**, 1342–1346.
- HOLNESS, M. B. & GRAHAM, C. M. 1995.  $P$ – $T$ – $X$  Effects on equilibrium carbonate– $\text{H}_2\text{O}$ – $\text{CO}_2$ – $\text{NaCl}$  dihedral angles: constraints on carbonate permeability and the role of deformation during fluid infiltration. *Contributions to Mineralogy and Petrology*, **119**, 301–313.
- HURTGEN, M. T., ARTHUR, M. A., SUITS, N. S. & KAUFMAN, A. J. 2002. The S isotopic composition of Neoproterozoic seawater sulfate: implications for a snowball Earth? *Earth and Planetary Science Letters*, **203**, 413–429.

## NEOPROTEROZOIC S-ISOTOPES AND GOLD VEINS

- HUSSEIN, A. & HIPKIN, R. E. 1981. *Bouguer Anomaly Map of the British Isles, Northern Sheet*. University of Edinburgh, Edinburgh.
- HUTTON, D. H. W. 1979. Tectonic slides: a review and reappraisal. *Earth Science Reviews*, **15**, 151–172.
- KAJIWARA, Y. & KROUSE, H. R. 1971. S-isotope partitioning in metallic sulfide systems. *Canadian Journal of Earth Science*, **8**, 1397–1408.
- KELLEY, S. P. & FALICK, A. E. 1990. High precision spatially resolved analysis of  $\delta^{34}\text{S}$  in sulfides using a laser extraction system. *Geochimica et Cosmochimica Acta*, **54**, 883–888.
- KENNEDY, M., DROSER, M., MAYER, L. M., PEVEAR, D. & MROFKA, D. 2006. Late Precambrian oxygenation; inception of the clay mineral factory. *Science*, **311**, 1446–1449.
- KNAUTH, I. P. & KENNEDY, M. J. 2009. The late Precambrian greening of the Earth. *Nature*, **460**, 728–732.
- KRABBENDAM, M., LESLIE, A. G., CRANE, A. & GOODMAN, S. 1997. Generation of the Tay Nappe, Scotland, by large-scale SE-directed shearing. *Journal of the Geological Society, London*, **154**, 15–24.
- KUZNETSOV, A. B. 1998. *Evolution of Sr composition in late Riphean seawater*. PhD thesis, Institute of Precambrian Geology and Geochronology, Russian Academy of Science.
- LAOUAR, R. 1987. *A S-isotope study of the Caledonian granite of Britain and Ireland*. Unpublished MSc thesis, University of Glasgow.
- LARGE, R. R., BULL, S. W. & MASLENNIKOV, V. V. 2011. A carbonaceous sedimentary source-rock model for Carlin-type and Orogenic gold deposits. *Economic Geology*, **106**, 331–358.
- LENTON, T. M. & WATSON, A. J. 2004. Biotic enhancement of weathering, atmospheric oxygen and carbon dioxide in the Neoproterozoic. *Geophysical Research Letters*, **31**, L05202, <http://dx.doi.org/10.1029/2003GL018802>
- LI, Y. & LUI, J. 2006. Calculation of S-isotope fractionation in sulfides. *Geochimica et Cosmochimica Acta*, **70**, 1789–1795.
- LOWRY, D. 1991. *The genesis of Late Caledonian granitoid-related mineralisation in Northern Britain*. Unpublished PhD thesis, University of St Andrews.
- LOWRY, D., BOYCE, A. B., FALICK, A. E. & STEPHENS, W. E. 1995. Genesis of porphyry and plutonic mineralisation systems in metaluminous granitoids of the Grampian Terrane, Scotland. *Transactions of the Royal Society of Edinburgh: Earth Science*, **85**, 221–237.
- LOWRY, D., BOYCE, A. J., FALICK, A. E., STEPHENS, W. E. & GRASSINEAU, N. V. 2005. Terrane and basement discrimination in northern Britain using S-isotopes and mineralogy of ore deposits. In: McDONALD, I., BOYCE, A. J., BUTLER, I. B., HERRINGTON, R. J. & POLYA, D. A. (eds) *Deposits and Earth Evolution*. Geological Society, London, Special Publications, **248**, 133–151.
- MACDONALD, F. A., JONES, D. S. & SCHRAG, D. P. 2009. Stratigraphic and tectonic implications of newly discovered glacial diamictite-cap carbonate couplet in southwestern Mongolia. *Geology*, **37**, 123–126.
- MCCAY, G. A., PRAVE, A. R., ALSOP, G. I. & FALICK, A. E. 2006. Glacial trinity: Neoproterozoic Earth history within the British–Irish Caledonides. *Geology*, **34**, 909–912.
- MELEZHIK, V. A., GOROKHOV, I. M., KUZNETSOV, A. B. & FALICK, A. E. 2001. Chemostratigraphy of Neoproterozoic carbonates: implications for ‘blind dating’. *Terra Nova*, **13**, 1–11.
- MERNAGH, T. P. & BIERLEIN, F. P. 2008. Transport and precipitation of gold in Phanerozoic metamorphic terranes from chemical modelling of fluid-rock interaction. *Economic Geology*, **103**, 1613–1640.
- MOLES, N. R. 1985. Metamorphic conditions and uplift history in central Perthshire: evidence from mineral equilibria in the Foss celsian-barite-sulfide deposit, Aberfeldy. *Journal of the Geological Society, London*, **142**, 39–52.
- MOLES, N. R., BOYCE, A. J. & FALICK, A. E. 2014. Abundant sulfate in the Neoproterozoic ocean: implications of constant  $\delta^{34}\text{S}$  of barite in the Aberfeldy SEDEX deposits, Scottish Dalradian. In: JENKIN, G. R. T., LUSTY, P. A. J., McDONALD, I., SMITH, M. P., BOYCE, A. J. & WILKINSON, J. J. (eds) *Ore Deposits in an Evolving Earth*. Geological Society of London, Special Publications, **393**, <http://dx.doi.org/10.1144/SP393.7>
- MOORE, P. 2011. *Developing an exploration guide for the auriferous breccia pipes at Beinn Udlaidh, Scotland*. Unpublished MGeol project. University of Leicester.
- MURCHISON, R. I. & GEIKIE, A. 1861. On the altered rocks of the Western Islands of Scotland and the North-western and Central Highlands. *Quarterly Journal of the Geological Society*, **17**, 171–232.
- NEILSON, J. C., KOKELAAR, B. P. & CROWLEY, Q. G. 2009. Timing, relations and cause of plutonic and volcanic activity of the Siluro-Devonian post-collision magmatic episode in the Grampian Terrane, Scotland. *Journal of the Geological Society, London*, **166**, 545–561.
- NESBITT, B. E. 1988. *Reconnaissance study of  $\delta^{34}\text{S}$  values of sulphides from mesothermal gold deposits of the Eastern Canadian Cordillera*. British Columbia Ministry of Energy, Mines and Petroleum Resources, Geological Fieldwork 1987, Paper **1988-1**.
- NOBLE, S. R., HYSLOP, E. K. & HIGHTON, A. J. 1996. High precision U–Pb monazite geochronology of the c. 806 Ma Grampian Shear Zone and the implications for the evolution for the Central Highlands of Scotland. *Journal of the Geological Society, London*, **153**, 511–514.
- OHMOTO, H. 1986. Stable isotope geochemistry of ore deposits. Chapter 14. In: VALLEY, J. W., TAYLOR, H. P., JR. & O’NEIL, J. R. (eds) *Stable Isotopes in High Temperature Geological Processes*. Mineralogical Society of America, Chantilly, VA. Reviews in Mineralogy, **16**, 491–559.
- OLIVER, G. J. H. 2001. Reconstruction of the Grampian episode in Scotland: its place in the Caledonian Orogeny. *Tectonophysics*, **332**, 23–49.
- OLIVER, G. J. H., WILDE, S. A. & WAN, Y. 2008. Geochronology and geodynamics of Scottish granitoids from the late Neoproterozoic break-up of Rodinia to Palaeozoic collision. *Journal of the Geological Society, London*, **165**, 661–674.
- PARNELL, J., BOYCE, A. J., MARK, D., BOWDEN, S. & SPINKS, S. 2010. Early oxygenation of the terrestrial

- environment during the Mesoproterozoic. *Nature*, **468**, 290–293.
- PATRICK, R. A. D., COLEMAN, M. L. & RUSSELL, M. J. 1983. Sulphur isotopic investigation of vein lead–zinc mineralisation at Tyndrum, Scotland. *Mineralium Deposita*, **18**, 477–485.
- PATRICK, R. A. D., BOYCE, A. & MACINTYRE, R. M. 1988. Au–Ag vein mineralisation at Tyndrum, Scotland. *Mineralogy and Petrology*, **38**, 61–76.
- PICKERING, K. T., BASSETT, M. G. & SIVETER, D. J. 1988. Late Ordovician–Early Silurian destruction of the Iapetus Ocean; Newfoundland, British Isles and Scandinavia; a discussion. *Transactions of the Royal Society of Edinburgh: Earth Sciences*, **79**, 361–381.
- PITCAIRN, I. K., TEAGLE, D. A. H., CRAW, D., OLIVIO, G. K., KERRICH, R. & BREWER, T. S. 2006. Sources of metals and fluids in orogenic gold deposits; insights from the Otago and Alpine schists, New Zealand. *Economic Geology*, **101**, 1525–1546.
- PLANT, J. A., STONE, P., FLIGHT, D. M. A., GREEN, P. M. & SIMPSON, P. R. 1997. Geochemistry of the British Caledonides: the setting for metallogeny. *Transactions of the Institute of Mining and Metallurgy: Section B Applied Earth Science*, **106**, B67–78.
- PLEWES, W. T. 2012. *Comparison of the main vein and northeast extension vein at Beinn Udlaidh and Coire Ghamhnain, for Scotgold's Gold Exploration Project, Tyndrum, Scotland*. Unpublished MGeol project. University of Leicester.
- PORTER, S. J. & SELBY, D. 2010. Rhenium–Osmium (Re–Os) molybdenite systematics and geochronology of the Cruachan granite skarn mineralisation, Etive complex: implications for emplacement chronology. *Scottish Journal of Geology*, **46**, 17–21.
- PRAYE, A. R., FALLICK, A. E., THOMAS, C. W. & GRAHAM, C. M. 2009. A composite C-isotope profile for the Neoproterozoic Dalradian Supergroup of Scotland and Ireland. *Journal of the Geological Society, London*, **166**, 845–857.
- PRINGLE, J. 1940. The discovery of Cambrian Trilobites in the Highland Border rocks near Callendar, Perthshire (Scotland). *Advancement of Science*, **1**, 252.
- RICE, C. M., MARK, D. F., SELBY, D. & HILL, N. J. 2012. Dating vein-hosted Au deposits in the Caledonides of N. Britain. Mineral Deposit Studies Groups meeting abstracts. *Transactions of the Institute of Mining and Metallurgy (Section B: Applied Earth Science)*, **121**, 199–200.
- ROBERTS, A. M. & TREAGUS, J. E. 1979. Stratigraphical and structural correlation between the Dalradian rocks of the SW and Central Highlands of Scotland. In: HARRIS, A. L., HOLLAND, C. H. & LEAKE, B. E. (eds) *The Caledonides of the British Isles*. Geological Society, London, Special Publications, **8**, 199–204.
- ROBINSON, B. W. & KASAKABE, M. 1975. Quantitative preparation of SO<sub>2</sub> for <sup>34</sup>S/<sup>32</sup>S analysis from sulfides by combustion with cuprous oxide. *Analytical Chemistry*, **47**, 1179–1181.
- ROGERS, G. & DUNNING, G. R. 1991. Geochronology of appinitic and related granitic magmatism in the W Highlands of Scotland: constraints on the timing of transcurrent fault movement. *Journal of the Geological Society, London*, **148**, 17–27.
- ROONEY, A. D., CHEW, D. M. & SELBY, D. 2011. Re–Os geochronology of the Neoproterozoic–Cambrian Dalradian Supergroup of Scotland and Ireland: implications for Neoproterozoic stratigraphy, glaciations and Re–Os systematics. *Precambrian Research*, **185**, 202–214.
- SCOTGOLD RESOURCES LIMITED 2010. *Drilling confirms further anomalous gold mineralisation in breccia pipes at Beinn Udlaidh*. ASX announcement, 17 February 2010.
- SCOTGOLD RESOURCES LIMITED 2011a. *Exploration update: River Vein and Beinn Udlaidh areas*. ASX announcement, 8 February 2011.
- SCOTGOLD RESOURCES LIMITED 2011b. *Exploration update: Auch project area*. ASX announcement, 19 January 2011.
- SCOTGOLD RESOURCES LIMITED 2012a. *Cononish Resource Update*. ASX announcement, 14 November 2012.
- SCOTGOLD RESOURCES LIMITED 2012b. *Sron Garbh Mafic complex*. ASX announcement, 7 March 2012.
- SCOTGOLD RESOURCES LIMITED 2012c. *Exploration progress at River Vein*. ASX announcement, 27 January 2012.
- SCOTT, R. A., PATRICK, R. A. D. & POLYA, D. A. 1987. *S isotopic and related studies on Dalradian stratabound mineralisation in the Tyndrum region, Scotland*. British Geological Survey Stable Isotope Report, **130**.
- SCOTT, R. A., PATRICK, R. A. D. & POLYA, D. A. 1991. Origin of sulphur in metamorphosed stratabound mineralisation from the Argyll Group, Dalradian of Scotland. *Transactions of the Royal Society of Edinburgh: Earth Science*, **82**, 91–98.
- SHIELDS, G. 1999. Working towards a new stratigraphic calibration scheme for the Neoproterozoic–Cambrian. *Eclogae Geologicae Helvetiae*, **92**, 221–233.
- SOPER, N. J. & HUTTON, D. H. W. 1984. Late Caledonian sinistral displacements in Britain – Implications for a 3-plate collision model. *Tectonics*, **3**, 781–794.
- SOPER, N. J., STRACHAN, R. A., HOLDSWORTH, R. E., GAYER, R. A. & GREILING, R. O. 1992. Sinistral transpression and the Silurian closure of Iapetus. *Journal of the Geological Society, London*, **146**, 871–880.
- SPENCE-JONES, C. P. 2013. *Metallurgical investigation of the ore from the Cononish Gold Deposit, Scotland*. Unpublished MGeol project. University of Leicester.
- STEPHENSON, D. & GOULD, D. 1995. *British Regional Geology: The Grampian Highlands*. HMSO, London.
- STEPHENSON, D., MENDUM, J. R., FETTES, D. J. & LESLIE, A. G. 2013. The Dalradian rocks of Scotland: an introduction. *Proceedings of the Geologists' Association*, **124**, 3–82.
- STRACHAN, R. A., SMITH, M., HARRIS, A. L. & FETTES, D. J. 2002. The Northern Highland and Grampian terranes. In: TREWIN, N. H. (ed.) *The Geology of Scotland*. The Geological Society, London.
- SUVOROVA, V. A. 1974. Temperature dependence of the distribution coefficient of S-isotopes between equilibrium sulfides. *National Symposium on Stable Isotope Geochemistry, 5th, Moscow, Program*, **1**, 128.
- TANNER, P. W. G. 2012. The giant quartz–breccia veins of the Tyndrum–Dalmally area, Grampian Highland, Scotland: their geometry, origin and relationship



# NEOPROTEROZOIC S-ISOTOPES AND GOLD VEINS

- to the Cononish Au–Ag deposit. *Transactions of the Royal Society of Edinburgh: Earth Science*, **103**, 1–26.
- TANNER, P. W. G. & SUTHERLAND, S. 2007. The Highland Border Complex, Scotland: a paradox resolved. *Journal of the Geological Society, London*, **164**, 111–116.
- TANNER, P. W. G. & THOMAS, P. R. 2009. Major nappe-like D2 folds in the Dalradian rocks of the Beinn Udlaidh area, Central Highlands, Scotland. *Transactions of the Royal Society of Edinburgh: Earth Science*, **100**, 371–389.
- THOMAS, C. W. 2000. *The petrology and isotope geochemistry of Dalradian carbonate rocks*. PhD thesis, University of Edinburgh.
- THOMAS, C. W., GRAHAM, C. M., ELLAM, R. M. & FALICK, A. E. 2004.  $^{87}\text{Sr}/^{86}\text{Sr}$  chemostratigraphy of Neoproterozoic Dalradian limestones of Scotland and Ireland: constraints on depositional ages and time scales. *Journal of the Geological Society, London*, **161**, 229–242.
- TILLEY, C. E. 1925. A preliminary study of the metamorphic zones in the Southern Highlands of Scotland. *Quarterly Journal of the Geological Society*, **81**, 100–112.
- TOMKINS, A. G. 2012. A biochemical influence of the secular distribution of orogenic Au. *Economic Geology*, **108**, 193–197.
- TREAGUS, J. E., PATTRICK, R. A. D. & CURTIS, S. F. 1999. Movement and mineralisation in the Tyndrum Fault Zone, Scotland and its regional significance. *Journal of the Geological Society, London*, **156**, 591–604.
- WAGNER, T., BOYCE, A. J. & FALICK, A. E. 2002. Laser combustion analysis of  $\delta^{34}\text{S}$  of sulfosalt minerals: determination of the fractionation systematics and some crystal-chemical considerations. *Geochimica et Cosmochimica Acta*, **66**, 2855–2863.
- WALTER, M. R., VEEVERS, J. J., CALVER, C. R., GORIAN, P. & HILL, A. C. 2000. Dating the 840–544 Ma Neoproterozoic interval by isotopes of strontium, carbon and sulfur in seawater, and some interpretative models. *Precambrian Research*, **100**, 371–433.
- WILLAN, R. C. R. 1996. Geochemistry of the Ben Eagach Schist, Dalradian Supergroup: Dispersion haloes from Aberfeldy-type hydrothermal centres? *Mineralisation in the Caledonides, Mike Gallagher Meeting*, Edinburgh, 27–28 June 1996, Abstract.
- WILLAN, R. C. R. & COLEMAN, M. L. 1983. S-isotope study of the Aberfeldy barite, zinc, lead deposit and minor sulfide mineralisation in the Dalradian metamorphic terrain, Scotland. *Economic Geology*, **78**, 1619–1656.
- WRIGHT, A. E. 1988. The Appin Group. In: WINCHESTER, J. A. (eds) *Later Proterozoic Stratigraphy of the Northern Atlantic regions*. Glasgow, Blackie.
- WRIGHT, A. E. & BOWES, D. R. 1968. Formation of explosion breccias. *Bulletin Volcanologique*, **32**, 15–32.